



Faculty of engineering

Department of chemical engineering

Master in hydrocarbon processing and engineering

TECHNICAL COMPARATIVE STUDY BETWEEN DIMETHYL ETHER AND
LIQUEFIED NATURAL GAS PRODUCTION FROM NATURAL GAS.

A Dissertation submitted to the faculty of engineering in partial fulfilment of the requirement
for the degree of Master of Science in Hydrocarbon processing engineering.

Student: Olive IRIBAGIZA

MAPUTO 2025



Faculty of engineering

Department of chemical engineering

Master in hydrocarbon processing and engineering

TECHNICAL COMPARATIVE STUDY BETWEEN DIMETHYL ETHER AND
LIQUEFIED NATURAL GAS PRODUCTION FROM NATURAL GAS.

A Dissertation submitted to the faculty of engineering in partial fulfilment of the requirement
for the degree of Master of Science in Hydrocarbon processing engineering.

Student: Olive IRIBAGIZA

Supervisor: Prof. Doutor João Chidamoio, Eng^o

MAPUTO 2025

DECLARATION OF DOCUMENT ORIGINALITY

I declare that this dissertation has never been submitted to obtain any degree or in any other context and is the result of my own individual work. This dissertation is presented in partial fulfillment of the requirements for the degree of Master of Science in Hydrocarbon Processing Engineering, from Universidade Eduardo Mondlane.

Olive IRIBAGIZA

ABSTRACT

The demand for energy has increased significantly. On the other hand, energy production suppliers are located in different and remote locations around the world. This requires efficient transport and storage of large-scale energy. Usually, large-scale is stored and transported in liquefied forms due to its reduced volume. However, liquid cryogenic storage loses some of its energy due to evaporation, called boil-off gas (BOG), which is called by change in temperature between storage medium and environment. This study examines the production of Dimethyl Ether (DME) and Liquefied Natural Gas (LNG) from natural gas, comparing boil-off gas (BOG) generation, energy intensities, and environmental impacts using dynamic simulation. Results from the simulation indicate a significantly higher BOG rate for LNG, with storage pressure increasing from 0.5 atm to 4.1 atm over 15 days, compared to a minimal increase from 23.4 atm to 23.7 atm for DME in the same period. This suggests that DME offers superior storage stability with lower evaporative losses. However, DME production was found to be more energy-intensive, with an energy consumption of 37.9 GJ/tonne compared to 2.07 GJ/tonne for LNG, and also generated higher CO₂ emissions, at 2.12 kg CO₂/kg of DME versus LNG emission of 1.16 kg CO₂/kg of LNG. These findings highlight a trade-off between the lower BOG rate of DME and its higher energy and environmental impacts. Thus, the choice between DME and LNG production pathways depends on the specific priorities of the application, whether it be minimizing evaporative losses or reducing energy consumption and emissions.

Keywords: Liquefied Natural gas, Dimethyl ether, Boil off gas, Energy intensity

RESUMO

A procura de energia aumentou significativamente. Por outro lado, os fornecedores de produção de energia estão localizados em locais diferentes e remotos em todo o mundo. Isto requer um transporte e armazenamento eficientes de energia em grande escala. Normalmente, o grande volume é armazenado e transportado na forma liquefeita devido ao seu volume reduzido. No entanto, o armazenamento criogénico líquido perde parte da sua energia devido à evaporação, denominada gás de ebulição (BOG), que é denominado pela variação de temperatura entre o meio de armazenamento e o meio ambiente. Este estudo examina a produção de Éter Dimetílico (DME) e Gás Natural Liquefeito (GNL) a partir de gás natural, comparando a geração de gás ebuliente (BOG), as intensidades energéticas e os impactos ambientais utilizando simulação dinâmica. Os resultados da simulação indicam uma taxa de BOG significativamente mais elevada para o GNL, com a pressão de armazenamento a aumentar de 0,5 atm para 4,1 atm ao longo de 15 dias, em comparação com um aumento mínimo de 23,4 atm para 23,7 atm para o DME no mesmo período. Isto sugere que o DME oferece uma estabilidade de armazenamento superior com menores perdas por evaporação. No entanto, verificou-se que a produção de DME é mais intensiva em energia, com um consumo de energia de 37,9 GJ/tonelada em comparação com 2,07 GJ/tonelada para o GNL, e também gerou emissões de CO₂ mais elevadas, de 2,12 kg CO₂/kg de DME versus emissões de GNL de 1,16 kg CO₂/kg de GNL. Estas conclusões destacam um compromisso entre a menor taxa de DME no BOG e os seus maiores impactos energéticos e ambientais. Assim, a escolha entre vias de produção de DME e GNL depende das prioridades específicas da aplicação, quer minimizando as perdas por evaporação, quer reduzindo o consumo de energia e as emissões.

DEDICATION

I dedicate this work:

- To my academic staff
- To my beloved parents, brothers and sisters.
- To my friends and relatives.

May God, bless you All.

ACKNOWLEDGEMENTS

First, I express my gratitude to almighty God our creator, who guided and enabled me to complete this final year project. I take this opportunity to express my deepest appreciation to my parents, brothers and sisters for their love, care, and moral and financial support during this project. I also express my gratitude to the government of Mozambique and the authorities of Universidade Eduardo Mondlane for their sponsorship support in terms of finance and knowledge that led me to the success during my studies. I would also like to express my gratitude to my friends, relatives and everyone whose participation through ideas and contribution led me to complete this project. Last but not least, I deeply thanks go to my classmates for their brotherhood and fellowship we shared during my academic studies.

May God, bless you All.

Table of Contents

1. Introduction	1
1.1 Background	1
1.2 Motivation	3
1.3 Research Problem.....	3
1.4 Research Limitations.....	4
1.5 Research Objectives	5
1.5.1 General Objective	5
1.5.2 Specific objectives	5
2. Literature Review	6
2.1. Natural gas.....	6
2.2. Dimethyl Ether Production from natural gas	9
2.2.1. Dimethyl ether indirect synthesis.....	11
2.2.2. Dimethyl ether direct synthesis.....	13
2.3. Uses of Dimethyl Ether	24
2.4. Liquefied Natural Gas Production Process	26
2.4.1. Liquefaction Principles	28
2.4.2. Cascade liquefaction process	28
2.4.3. Mixed refrigerant liquefaction processes.....	30
2.4.4. Expansion-based processes	33
2.4.5. Comparison of the liquefaction technologies	34

2.5.	Liquefied natural gas storage, transportation and boil-off gas	35
2.5.1.	Boil-off rate.....	37
2.5.2.	Recovery of boil-off gas	39
3.	Research Methods.....	41
3.1.	Simulation model development.....	42
3.1.1.	Dimethyl ether Production Process.....	42
3.1.2.	Liquefied Natural Gas Production Process	45
3.1.3.	Boil Off Gas Estimation.....	48
4.	Results and Discussion	50
4.1.	Dimethyl Ether Production Process	50
4.2.	Liquefied Natural Gas Production Process	52
4.3.	Energy intensities and Greenhouse Gas Emission Comparison.....	54
4.3.1.	Energy analysis of dimethyl ether production	54
4.3.2.	Energy analysis for the liquefied natural gas production.....	56
4.4.	Boil off gas production comparison	57
5.	Conclusion and Recommendations	61
5.1.	Conclusion.....	61
5.2.	Recommendations	62
	References.....	63

LIST OF ABBREVIATIONS

ATR	Autothermal Reformer
BOG	Boil of Gas
CCS	Carbon Capture and Storage
DME	Dimethyl Ether
DMR	Dual Mixed Refrigerant
EOS	Equation of State
FCV	Flow Control Valve
FIC	Flow Indicator Controller
HC	Hydrocarbons
JBOG	Jetty Boil-off Gas
LCV	Level Control Valve
LIC	Level Indicator Controller
LNG	Liquefied Natural Gas
LPG	Liquefied Petroleum Gas
MCHE	Main Cryogenic Heat Exchanger
MR	Mixed Refrigerant
NG	Natural Gas
NGL	Natural Gas Liquids
NO _x	Nitrogen Oxides
PCV	Pressure Control Valve
PID	Proportional Integral Derivative
POX	Partial Oxidation
PR-EOS	Peng-Robinson Equation of State
PSA	Pressure Swing Adsorption
PV	Process Variable
S	Steam
SMR	Steam Methane Reforming
So _x	Sulphur Oxides
SR	Steam Reforming
TBOG	Tankage Boil-off Gas

NOMENCLATURE

r	Rate of Reaction
p	Partial Pressure, [bar]
K	Equilibrium Constant
k	Kinetic constant, [Kmol bar ^{0.5} kgcat ⁻¹ h ⁻¹]
ρ_s	Particle Density, [kg/m ³]
ρ_B	Bulk Density, [kg/m ³]
f	Fugacity, [bar]

LIST OF FIGURES

Figure 1: Natural gas processing: streams and final products.	8
Figure 2: Schematic overview of natural gas industry	9
Figure 3: DME Feedstock breakdown.	10
Figure 4: DME production Routes.....	11
Figure 5: Indirect DME production scheme	12
Figure 6: General Direct DME Production Scheme.	13
Figure 7: Pre-treatment of natural gas	14
Figure 8: ATR reactor scheme	15
Figure 9: Direct DME production scheme	19
Figure 10: DME synthesis and purification process scheme.	24
Figure 11: DME feedstocks and common applications	25
Figure 12: LNG supply chain	27
Figure 13: Pure refrigerant cascade process	29
Figure 14: Mixed refrigerant (MR) cascade process	29
Figure 15: Single Mixed Refrigerant Diagram.	31
Figure 16: DMR process diagram.....	32
Figure 17: C3-MR process diagram.....	32
Figure 18: Typical N2 expansion process diagram.....	33

Figure 19: LNG cooling curve of Cascade, MR and EXP	34
Figure 20: LNG receiving terminal	36
Figure 21: Heat ingress in LNG tank	38
Figure 22: BOG Recovery system	39
Figure 23: Dimethyl ether production and storage process flow diagram.....	44
Figure 24: Liquefied Natural Gas Production (C3MR) and Storage Train.	46
Figure 25: Boil-of gas train (dynamic simulation). The same scheme is valid for DME boil-of gas estimation.....	49
Figure 26: DME vapor stream concentration profile.....	50
Figure 27: DME liquid composition profile.	51
Figure 28: MCHE - 1 composite curves.	52
Figure 29: MCHE - 2 composite curves.	53
Figure 30: DME production process energy and GHG analysis.....	55
Figure 31: LNG production process energy and GHG analysis.	57
Figure 32: LNG boil off gas production.	58
Figure 33: DME boil off gas production.....	58
Figure 34: Simulation and experiments result in MCHE -1	60
Figure 35: Simulation and experiment results in MCHE -2	60

LIST OF TABLES

Table 1: Physical Property of DME and other fuels	10
Table 2: Kinetic Parameters of SMR.	18
Table 3: DME kinetic model parameters.	22
Table 4: DME synthesis operational conditions.	22
Table 5: LNG technologies comparison.	35
Table 6: Natural gas composition	43
Table 7: Mixed Refrigerant composition	47
Table 8: Storage tank properties and geometry	49

CHAPTER I

1. INTRODUCTION

1.1 BACKGROUND

The need for efficient transport and storage of large-scale energy is rising due to increase in demand for energy worldwide. On the other hand, energy production suppliers are located far away from the regions in demand around the world. This requires efficient transport and storage of large-scale energy. Usually, large-scale energy is stored and transported in liquefied forms due to its reduced volume. However, liquid cryogenic storage loses some of its energy due to evaporation, called boil-off gas (BOG), which is caused by a change in temperature between the storage medium and the environment.

Natural gas (NG) is a mixture of light hydrocarbons. It comprises methane, ethane, propane, butane, natural gasoline (C₅₊ cut) and some content of non-hydrocarbons components, which can be liquefied to produce the so known Liquefied Natural Gas (LNG). This product is widely taken as the future of the energy storage. In the other hand, dimethyl ether (DME) is non-toxic and non-carcinogenic chemical compound with physical characteristics closer to LPG, thus making it a potential energy carrier.

The scholar have proposed different energy carriers to store and transport large energy in liquefied form. Even though these energy carriers store and transport more energy compared to other forms of energy, storage and transportation processes in liquefied form loses some of its mass due of temperature difference between the environment and the storing device. These losses from energy carriers in liquefied form are called boil-off gas (BOG). The BOG occurs wat different stages of an energy carrier supply chain, but mainly at the onshore storage and maritime transportation phases (Al-Breiki & Bicer, 2020).

In the open literature there are many studies focusing on direct conversion of methane to DME as way of eliminating the flaring of natural gas. This would avoid burning methane in oil platforms, allowing the safe transportation of the natural gas in the form of DME. Researches made by Otaraku & Onyekaonwu (2018), Makos et al. (2019) and Jafariet al. (2021) discusses

the idea and existing technology to convert natural gas into DME as way of safe transporting of this commodity to avoid flaring.

As mentioned above, the major problem of both DME and LNG as energy carriers is the BOG formation. This losses impact both the calorific of the carriers as well a loss in mass. Al-Breiki & Bicer (2020) conducted research investigating the effect of BOG on energy carriers (methanol, LNG and DME) during land storage and maritime transportation. Their study focused on the loss of mass of DME and LNG due to energy intakes when storing these commodities. However, one should note that these researches present in the open literature mainly focus on the technical feasibility in terms of BOG generation only. These leaves room to make a more detailed analysis.

The global energy landscape stands at a critical point, considering the complex interplay between energy demand, environmental concerns, and the search for sustainable energy alternatives. Natural gas, a versatile and abundant hydrocarbon resource, has gained prominence as a transitional fuel due to its relatively lower carbon intensity compared to other fossil fuels such as coal and oil. Within this context, exploring and optimizing the production processes of derivative fuels like Dimethyl Ether (DME) and Liquefied Natural Gas (LNG) from natural gas emerges as a pivotal research domain.

DME, known for its properties as a clean-burning and versatile fuel, holds promise in various sectors, including transportation and power generation. Meanwhile, LNG remains a fundamental resource in the global energy trade due to its high energy density and ease of transportation. Understanding the technical issues of producing these derivatives from natural gas and evaluating their boil-off gas and energy intensity becomes imperative for informed decision-making regarding their industrial-scale adoption.

This dissertation aims to delve into a comparative study of the technical feasibility, specifically focusing on the boil-off gas and energy intensity aspects, pertaining to DME and LNG production processes. The utilization of Aspen HYSYS simulation software serves as a robust framework for modeling and evaluating these processes.

1.2 MOTIVATION

The state-of-the-art of the literature regarding LNG and DME technical feasibilities in terms of energy carriers, focus only on the comparison of the BOG rate of the two commodities, as mentioned in the last section. However, to make an educated choice between DME and LNG as energy carriers, a broader analysis should be made, comparing the entirety of factors that affect their feasibility. This includes an analysis covering the BOG generation rate, the environmental impacts, the energy intensities and economic feasibility study.

Due to these limitations present in the current open literature regarding this topic, there is a need to conduct more studies to cover the areas not explored up to now. Thus, the outcomes of this study are expected to provide critical insights into the technical feasibility of DME and LNG production, particularly concerning their boil-off gas generation, energy intensity and carbon footprint (CO₂ emissions). By elucidating the comparative advantages and challenges of these processes, this research aims to inform policymakers, industry stakeholders, and researchers about the optimal pathways for maximizing efficiency and sustainability in the utilization of natural gas-derived fuels.

In summary, this dissertation endeavors to contribute to the academic community by presenting a comprehensive comparative analysis of DME and LNG production processes, with a specific focus on their boil-off gas generation and energy intensity, ultimately aiming to guide informed decision-making in the global energy landscape.

1.3 RESEARCH PROBLEM

The contemporary energy scenario demands an in-depth exploration into the technical feasibility aspects of DME and LNG production, particularly concerning boil-off gas generation and energy intensity. The challenge lies in comprehensively understanding and comparing these two derivatives' production processes to ascertain their efficiency in utilizing natural gas feedstock. Addressing this requires a thorough investigation into the intricacies of boil-off gas dynamics and the energy intensities associated with the production pathways of DME and LNG. To navigate the complexities surrounding DME and LNG production, the following research questions will guide this study:

1. What are the boil-off gas generation profiles within the DME and LNG production processes, and how do these compare in terms of quantity and management strategies?
2. How do the energy intensities of DME and LNG production differ concerning resource utilization and operational efficiency?
3. What are the key technical factors influencing the comparative feasibility of DME and LNG production, particularly in the context of boil-off gas dynamics and energy intensity?

1.4 RESEARCH LIMITATIONS

While this study aims to delve deeply into the technical feasibility of DME and LNG production, certain limitations exist: factors such as economic feasibility and broader environmental impact assessments are beyond the immediate scope of this research and may warrant further investigation in subsequent studies.

1.5 RESEARCH OBJECTIVES

1.5.1 GENERAL OBJECTIVE

To conduct a comprehensive comparative analysis that assesses the technical feasibility of DME and LNG production processes.

1.5.2 SPECIFIC OBJECTIVES

- To develop a model and simulate the production processes of DME and LNG derived from natural gas feedstock;
- To investigate a comprehensive understanding of the difference in boil-off gas generation between DME and LNG;
- To evaluate the energy intensities of DME and LNG production, focusing on resource efficiency and optimizing energy consumption.

CHAPTER II

2. LITERATURE REVIEW

The use of alternative fuels has become a crucial topic of research in the field of sustainable energy solutions. In order to conduct a technical comparison between DME and LNG, which is both created from natural gas, this chapter reviews critically the state-of-the-art of DME and LNG productions. The inquiry looks into essential features critical for evaluating the practicality and sustainability of these alternative fuels, with a particular emphasis on Boil-Off Gas (BOG) management, energy intensity, and CO₂ emissions. This review attempts to clarify the complex technical nuances and relative benefits of employing DME and LNG as sources for clean energy.

2.1 NATURAL GAS

Natural gas (NG) is a mixture of light hydrocarbons. It comprises methane, ethane, propane, butane, natural gasoline (C₅₊ cut) and some content of non-hydrocarbons components, such as oxygen, nitrogen, sulphur, mercury, helium and chlorine, which are also known as heteroatoms. NG as it occurs in nature it cannot be used, due to the high level of impurities within it, mostly coming from the heteroatoms. The heteroatoms of NG, have no intrinsic calorific value; thus, their presence in the NG stream reduce (as consequence of dilution) the calorific value of the hydrocarbons contents of NG. Finally but not least important, these heteroatoms are deleterious for the NG processing, since they are the main source for catalyst deactivation.

Gas condensate is a hydrocarbon liquid stream separated from natural gas and consists of higher-molecular-weight hydrocarbons that exist in the reservoir as constituents of natural gas. Gas condensate are recovered as liquids in the wellhead separators as the pressure declines during NG production at the processing plants. The condensate stream is composed by ethane, propane, butane, and natural gasoline (C₅₊ cut). There is a specific terminology used in the natural gas processing industry for this liquid hydrocarbon stream recovered from natural, i.e all condensates; C₂ to C₈ are natural gas liquids (NGL). Natural gas liquids must not be confused with Liquefied Petroleum Gas (LPG); LPG, is a fraction of the NGL comprising only of propane and butane, with some amounts of ethane, pentanes and iso-butanenes as impurities (Speight, 2015).

The two primary uses for natural gas are as a fuel and as a petrochemical feedstock, however, before that happens, NG undergoes a pre-treatment process, comprised by the following steps:

- Purification - removal of materials, valuable or not, that inhibit the use of the gas as an industrial or residential fuel;
- Separation - splitting out of components that have greater value as petrochemical feedstocks, standalone fuels (e.g., propane), or industrial gases (e.g., ethane, helium);
- Liquefaction - increase of the energy density of the gas for storage or transportation.

Typical pre-treatment processes for Natural Gas in a natural gas processing plant are depicted in Figure 1. In any natural gas processing plants the objective is to treat the raw gas brought in from the field so that it can be sold to downstream users. Natural gas treatment steps shown in figure 1 may depend on natural gas composition or sales specification. Three to four basic processing steps are common in the gas processing plants on order to bring the raw gas at the wellhead up to either plant or sale specifications:

1. Condensate and water removal: this involves separating the gas from free liquids such as water, crude oil, LPG condensate and entrained solids;
2. Acid gas removal or gas sweetening: remove undesirables such as sour components, such as carbon dioxide and hydrogen sulphide; The sour components separated (mainly H₂S and CO₂) from the gas can be converted to elemental sulphur (Claus process) which in turn is sold for downstream customers' use or flared to atmosphere depending on environmental requirements;
3. Water removal or dehydration: processing of gas to remove water vapor.

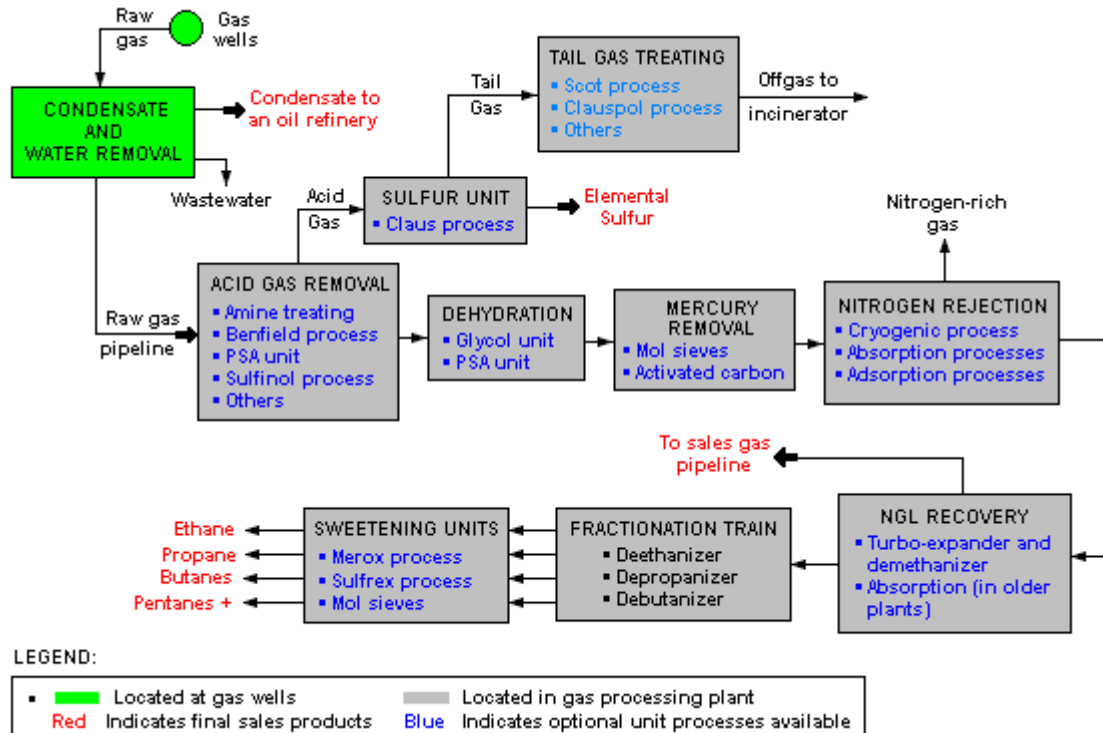


Figure 1: Natural gas processing: streams and final products. Adapted from Petro blogger (2011).

After appropriate removal of impurities and separation of valuable hydrocarbons, natural gas is sent to petrochemical industry as feedstock for production for instance Of DME, LNG, or other used as shown in figure 2. Alternatively, processed natural gas is transported via pipeline to the market. Natural gas transportation via pipeline usually impose restrictions on the make-up of the natural.

Figure 2 shows a simplified flow of material from reservoir to finished product and provides an overall perspective of natural gas value chain.

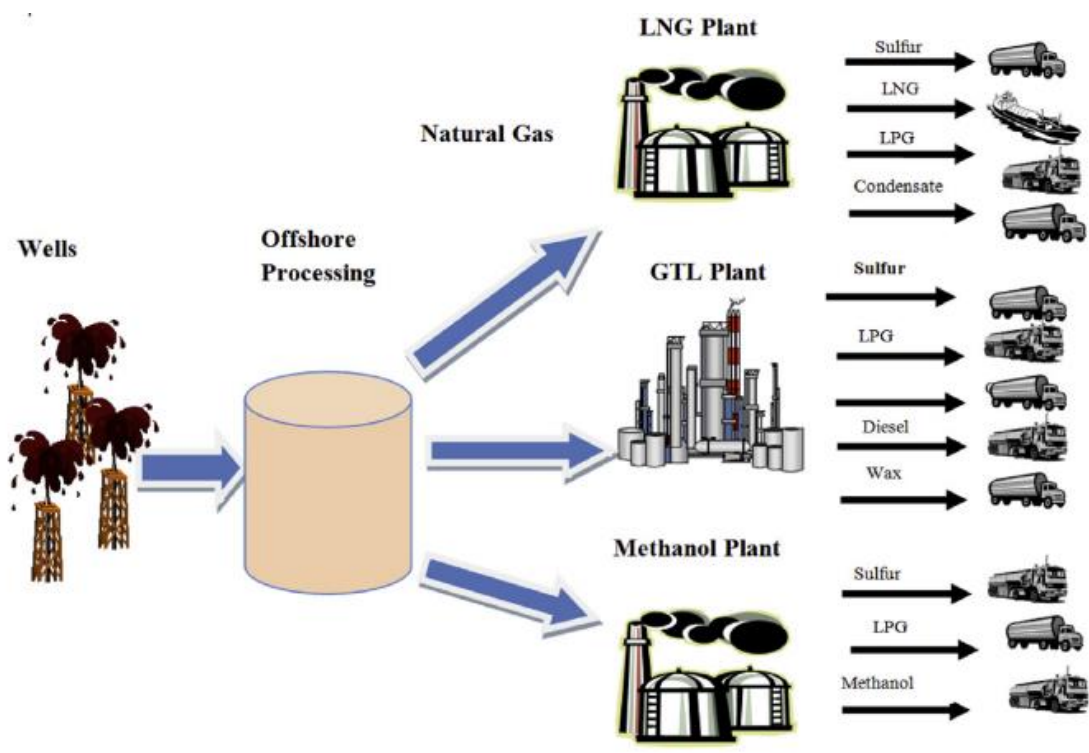


Figure 2: Schematic overview of natural gas industry (Kelechi et al., 2022)

The next sections discuss the production of DME and LNG from natural gas as standalone processes.

2.2 DIMETHYL ETHER PRODUCTION FROM NATURAL GAS

The basic ether is the dimethyl ether (DME) with the chemical formula CH_3OCH_3 , is non-toxic and non-carcinogenic. The Hydrogen/Carbon ratio, H/C ratio, is high and it lacks Carbon-Carbon, C-c bonds. Because DME and LPG share comparable physical characteristics, DME can be delivered and stored utilizing current infrastructures with just minor adjustments. DME is therefore thought to be an alternative to LPG for heating and cooking, as well as for use as an aerosol propellant in spray cans. Because DME has a high cetane number and produces fewer NO_x emissions when burned, it is also regarded as a diesel fuel substitute (Karagoz, 2014). It is a colorless gas, sulfur and nitrogen free. Selected physical properties and combustion characteristics of DME compared with other relating fuels are presented in Table 1. The vapor pressure of DME is about 0.6 MPa at 25° C, which means that DME liquefies easily under light pressure (Ogawa et al., 2004).

DME does not require expensive LNG tankers or LNG facilities for storage because it may be distributed and stored using LPG handling technology. After natural gas is transformed into DME, it will offer a competitive alternative method of natural gas transportation (Ogawa et al., 2004).

DME can be produced from different sources (see Figure 3) such, crude oil, residual oil, coal, waste products and biomass.

Table 1: Physical Property of DME and other fuels (Ogawa et al., 2004)

[Properties]	DME	Propane	Methane	Methanol	Diesel
Chemical formula	CH ₃ OCH ₃	C ₃ H ₈	CH ₄	CH ₃ OH	-
Boiling point (K)	247.9	231	111.5	337.6	180-370
Liquid density (g/cm ³ , 293K)	0.67	0.49	-	0.79	0.84
Specific gravity (vs. air)	1.59	1.52	0.55	-	-
Vapor pressure (atm, 293K)	6.1	9.3	-	-	-
Explosion limit	3.4-17	2.1-9.4	5-15	5.5-36	0.6-6.5
Cetane number	55-60	(5)	0	5	40-5
Net calorific value (MJ/Nm ³)	59.44	91.25	36.0	-	-
Net calorific value (MJ/kg)	28.90	46.46	50.23	21.1	41.86

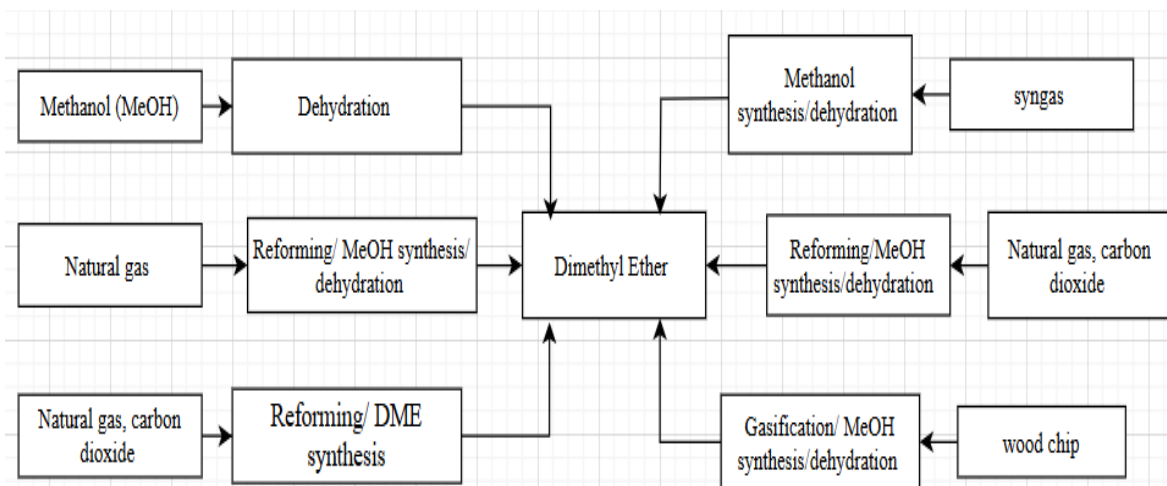


Figure 3: DME Feedstock breakdown.

However, DME production can be taken in two different ways, the direct route, where DME is directly produced from syngas and the indirect route which involves the upstream methanol production (Fortin et al., 2020), see Figure 4. Direct DME production process consists of pretreatment, reforming, gas cleaning-recycles, DME synthesis, and separation and purification of DME sections (Karagoz, 2014).

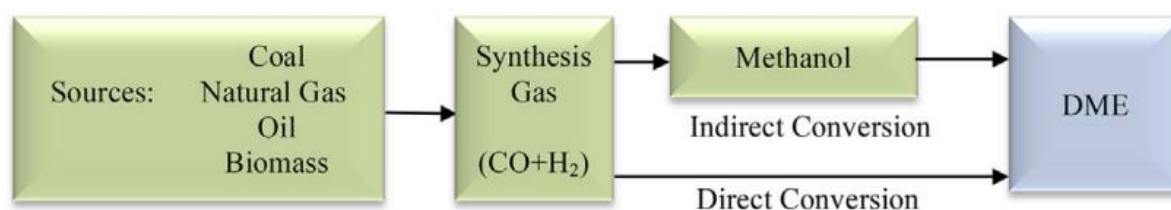


Figure 4: DME production Routes.

2.2.1 DIMETHYL ETHER INDIRECT SYNTHESIS

DME can be produced in two different ways, as previously mentioned and illustrated in Figure 4. The first method, known as the indirect route, uses the produced methanol to promote its dehydration in separated reactors, while the second, and possibly more efficient, method is known as the direct route and involves the single-stage production of DME using bi-functional catalysts.

The technology of this one step process belongs to companies such as Haldor Topsoe, JFE Holdings, Korea Gas Corporation, Air Products, and NKK (Azizi et al., 2014).

DME has traditionally been made from syngas using a two-step process in which methanol is first generated, refined, and then transformed into DME in a second reactor. The following equation illustrates how a dehydration process converts methanol to DME (Fortin et al., 2020).



The manufacture of DME is theoretically preferred at low temperatures since the dehydration of methanol to DME is an exothermic process. It occurs in the presence of solid-acid catalysts such as $\gamma\text{-Al}_2\text{O}_3$, zeolites, or silica-modified alumina. Figure 5 describes a typical indirect DME production scheme.

The production scheme depicted in Figure 5 starts with methanol that is produced from natural gas steam reforming. As matter of simplification, the reforming section has not been presented down below.

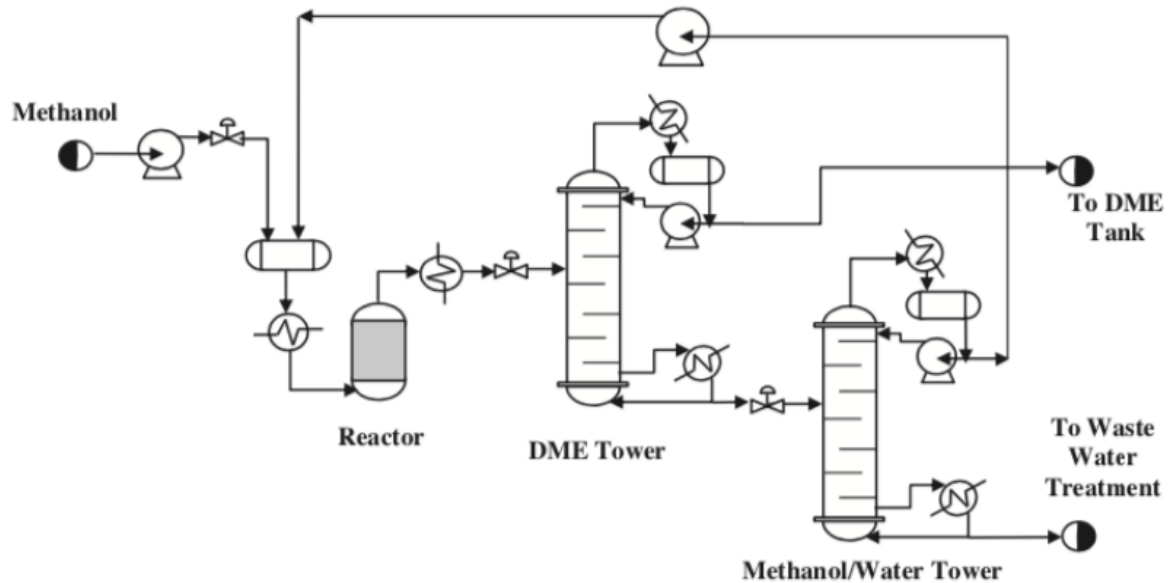


Figure 5: Indirect DME production scheme (Fortin et al., 2020)

A slightly altered indirect process is used to model the production of DME. Figure 5 displays the flowsheet for the fundamental indirect process. In this work, a methanol/ethanol mixture rather than pure methanol is used to feed the process. In fact, this lowers the feedstock's cost. Therefore, a first distillation of the process input stream is required to separate methanol and ethanol. After that, the ethanol is put away to be used later to make diethyl ether. However, the following study is restricted to the DME production process following methanol and ethanol separation.

2.2.2 DIMETHYL ETHER DIRECT SYNTHESIS

Recently, a technique for direct synthesis has been created. It entails converting syngas to dimethyl ether (DME) in a single step. This process flowsheet is shown in Figure 6. The operational units are those generally used for the purification and separation of the DME process. Using absorption, flash, and distillation, it enables the recovery of methanol and the separation of CH_4 , CO , N_2 , and H_2 . It makes it possible to produce a very pure DME product (Fortin et al., 2020).

Direct DME production process consists of pretreatment, reforming, gas cleaning-recycles, DME synthesis, and separation and purification of DME sections.

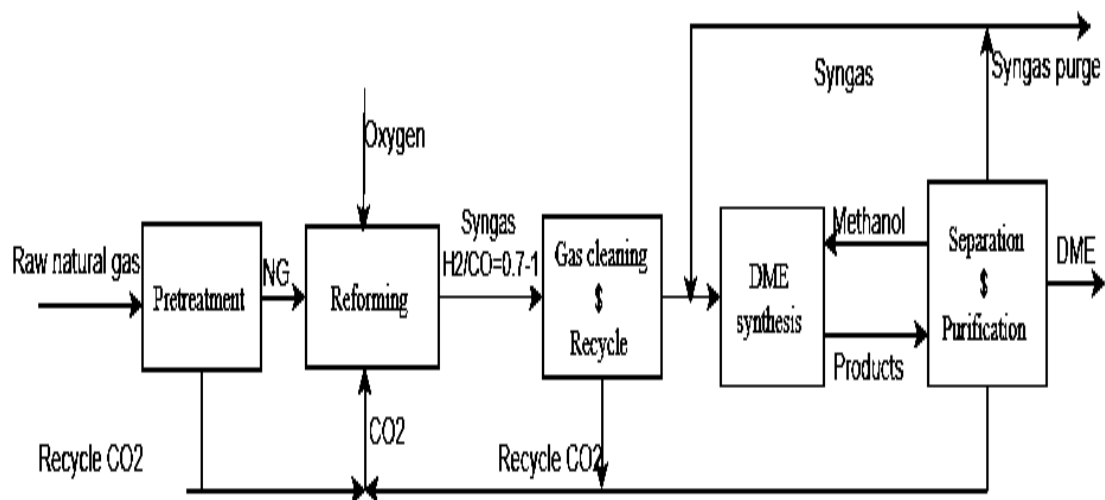


Figure 6: General Direct DME Production Scheme.

2.2.2.1 Pre-treatment Section

The purification of raw natural gas is the initial stage in the manufacturing of DME from it. Raw natural gas is initially delivered to an acid-gas removal unit, as seen in Figure 7, and the dehydration process comes after. The membrane separation process continues with the nitrogen removal unit as the following stage. To recover natural gas liquids, the cooled nitrogen-reduced stream is transferred to a de-methanizer and subsequently a de-ethanizer (Karagoz, 2014). The pretreatment steps are similar as those described in subsection 1.6 figure 1.

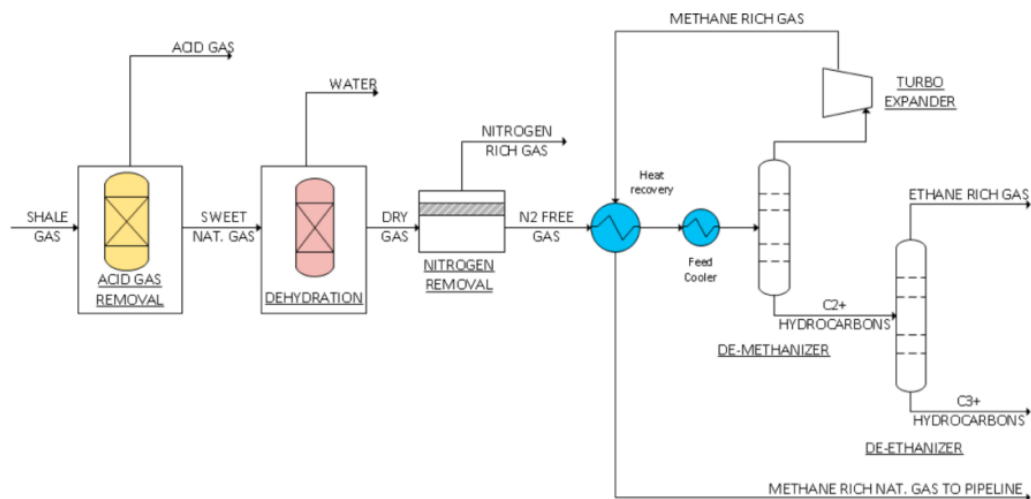


Figure 7: Pre-treatment of natural gas (Karagoz, 2014)

2.2.2.2 Reforming Section

The natural gas is sent to a fractionation plant in the pre-treatment phase shown in Figure 7 in order to produce liquid light hydrocarbons and methane-rich gas, which are frequently utilized as feedstocks in the petrochemical industries. The demethanizer recovers the gas that is rich in methane. After that, the reforming section receives the methane-rich gas in order to produce DME.

Natural gas is the main source in industry to produce syngas. There are mainly four types of reforming: Autothermal reforming (ATR), steam methane reforming (SMR), dry reforming, and combinations of these reforming. Process objectives, availability of material, energy resources, final product, energy requirement, environmental issues and safety issues are the main concepts for selection of reforming type or types (Noureldin et al., 2014).

ATRs are attractive when used in combination with a reforming exchanger. They are also suited for making large volumes of synthesis gas, especially with relatively low hydrogen/carbon monoxide ratios such as 1.5/1 – 3/1. These lower ratios are desirable for synthesis of higher molecular weight hydrocarbons (Rice & Mann, 2007), such as DME.

In the past 10 years, pre-reformers have become more significant in the industry. An adiabatically operating catalyst-filled vessel is called a pre-reformer. The heat of reaction is provided by the entering reactants, which have varying heat contents. The feed's higher hydrocarbons are transformed to methane along with a negligible quantity of hydrogen and

carbon oxides. Pre-reformers are used to handle variations in the composition of natural gas, debottleneck already-existing primary reformers, and transform heavy feedstocks into methane and lighter components (Franceus et. al., 1999).

A schematic with flow streamlines is pictured in Figure 8.

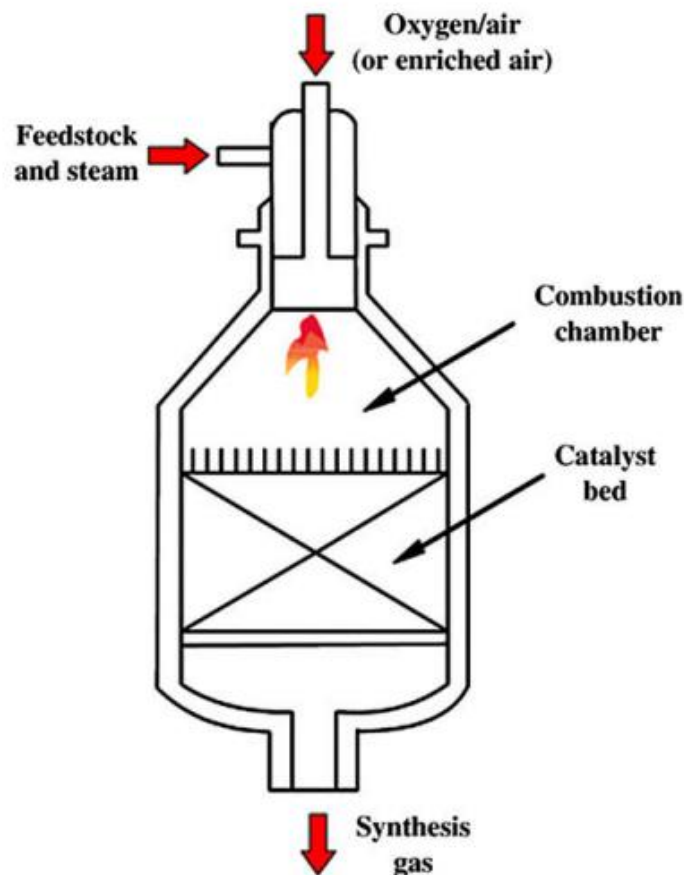


Figure 8: ATR reactor scheme (Zahedi nezhad et al., 2009)

An ATR reactor has a bed loaded with catalyst at the bottom and a combustion zone at the top. In the combustion zone, the feedstock is combined with a sub-stoichiometric volume of oxidant and burnt. The heated gases continue to react in an intermediate conical recirculation section, in the bottom part, the resulting gases are passed over the catalyst in an attempt to create a mixture of water as close to equilibrium as possible. To achieve the low end of the H_2/CO range, recycle of carbon dioxide is required (Rice & Mann, 2007).

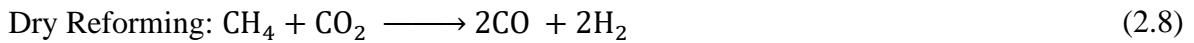
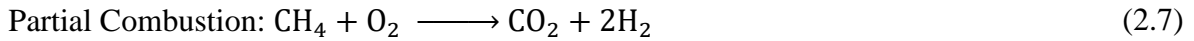
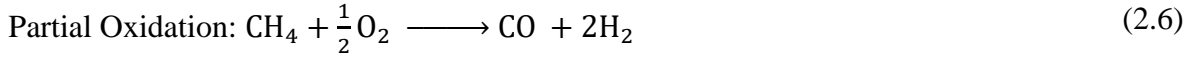
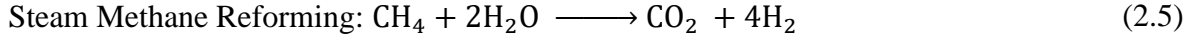
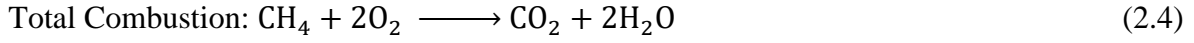
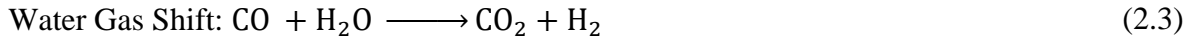
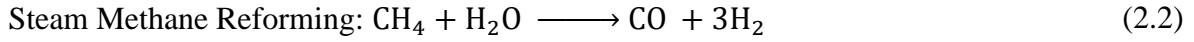
The feedstock and Oxygen/air are mixed and fed to the combustion chamber through the installed burner and ignite. Partial combustion reactions occur (POX reactions) and flame

temperatures over 3000 °C can be achieved. The high temperatures promote SR reactions in homogeneous phase and decrease gas temperatures due to their endothermic heat of reaction; gas temperatures at catalyst bed inlet reach 1100-1300 °C. The gas mixture at the inlet of the catalyst section is composed of hydrogen, carbon monoxides, steam and unconverted hydrocarbons. At this low temperature homogeneous SR reactions no longer occur and the catalyst becomes essential for the heterogeneous SR reactions. The catalyst section brings the mixture to equilibrium, and also stabilizes the syngas by removing any soot precursors formed in the combustion chamber; gas outlet temperatures are typically in the range of 900-1100 °C (Manaças, 2013).

Both pure oxygen and (enriched) air can be employed as the oxidant, and both has benefits and drawbacks. With air fueled ATR, the air separation unit, which represents for 30–40% of plant capital costs, is eliminated. However, bigger equipment, greater compression duties, and a once-through operation are still required. ATR powered by oxygen will need an air separation unit, although operating expenses will generally compensate it. Air-blown ATR is only utilized when the syngas requires nitrogen, like in the case of producing ammonia. Natural gas reformation by ATR can produce lower H₂/CO output ratios (1.8–3.8) than SMR because oxygen is introduced in place of steam (Seungjune et al., 2008).

Compared to SMR, typical working pressures for oxygen-blown ATR can reach 40–50 bar, which can compensate for the unfavorable pressure effect on methane conversion by reaching higher temperature. Sub-stoichiometric oxygen feeding conditions are often achieved at oxygen to methane ratios (O₂/C ratios) of 0.5–0.6. Less steam is needed for carbon-free operation, which corresponds to an S/C ratio of less than 1. Typically, 16 mm diameter and 8–10 mm height hollow ring-shaped catalyst pellets, or Ranching rings, are utilized in ATR. Alumina support contains 3-12% nickel. These catalysts are made with a minimal pressure drop to prevent process gas bypassing, excellent temperature stability, and enough activity to attain equilibrium (Manaças, 2013).

Numerous reactions are expected to happen during the reforming process of natural gas. The series of reactions shown below, will occur if methane is thought to be the primary dominant specie in natural gas (Azarhoosh et al., 2015).



To reduce the complexity in the development and solution of the simulation model, only the reactions with significant rates will be considered. The first three reactions prove to have significant rates, from Equations 2.2, 2.3 e 2.4 (Numaguchi & Kikuchi, 1988). Therefore, other reactions were ignored in this modeling study.

Xu & Froment (1989), present a very accepted modelling for the kinetics of SMR reactions in the literature. In their study, the SMR reactions are described using the following kinetic equations, for reactions 2.2 and 2.3, respectively:

$$r_2 = \frac{k_1}{p_{\text{H}_2}^{2.5}} \left(p_{\text{CH}_4} p_{\text{H}_2\text{O}} - \frac{p_{\text{H}_2}^3 p_{\text{CO}}}{K_1} \right) / (\text{DEN})^2 \quad (2.11)$$

$$r_3 = \frac{k_2}{p_{\text{H}_2}} \left(p_{\text{CO}} p_{\text{H}_2\text{O}} - \frac{p_{\text{H}_2} p_{\text{CO}_2}}{K_2} \right) / (\text{DEN})^2 \quad (2.12)$$

$$\text{DEN} = 1 + K_{\text{CO}} p_{\text{CO}} + K_{\text{H}_2} p_{\text{H}_2} + K_{\text{CH}_4} p_{\text{CH}_4} + K_{\text{H}_2\text{O}} p_{\text{H}_2\text{O}} / p_{\text{H}_2} \quad (2.13)$$

The kinetic constants of this rate equations are summarized in Table 2. The catalyst used by Xu and Froment (1989) had the following specifications: the catalyst contained 15.2% nickel, supported on magnesium spinel. Its BET-surface area was 58 m², the nickel surface area 9.3 m²/g, (fresh catalyst) and the void fraction of 0.528. The original ring-shaped catalyst with outer diameter of 10 mm was crushed into particles of 0.18-0.25 mm.

Table 2: Kinetic Parameters of SMR.

Parameter	Expressions	Dimensions	Source
k_1	$k_1 = 4.225 \times 10^{15} e^{\left(\frac{-240.1}{RT}\right)}$	Kmol bar ^{0.5} kgcat ⁻¹ h ⁻¹	Xu and Froment (1989)
k_2	$k_2 = 1.995 \times 10^6 e^{\left(\frac{-67.1}{RT}\right)}$	Kmol bar ⁻¹ kgcat ⁻¹ h ⁻¹	Xu and Froment (1989)
K_{CO}	$K_{CO} = 8.23 \times 10^{-5} e^{\left(\frac{70.65}{RT}\right)}$	bar ⁻¹	Xu and Froment (1989)
K_{H_2}	$K_{H_2} = 6.12 \times 10^{-9} e^{\left(\frac{82.90}{RT}\right)}$	bar ⁻¹	Xu and Froment (1989)
K_{CH_4}	$K_{CH_4} = 6.65 \times 10^{-4} e^{\left(\frac{38.28}{RT}\right)}$	bar ⁻¹	Xu and Froment (1989)
K_{H_2O}	$K_{H_2O} = 1.77 \times 10^5 e^{\left(\frac{-88.68}{RT}\right)}$	bar ⁻¹	Xu and Froment (1989)
K_{eq1}	K_{eq1} $= 1.198 \times 10^{15} e^{\left(\frac{-223064.62}{RT}\right)}$	[bar] ²	Hou and Hughes (2001)
K_{eq2}	$K_{eq2} = 1.767 \times 10^{-2} e^{\left(\frac{36581.6}{RT}\right)}$	[bar] ⁰	Hou and Hughes (2001)
$K_{1,1}$	$3.527 e^{\left(\frac{222824.52}{RT}\right)}$	Kmol bar ^{-1.5} kgcat ⁻¹ h ⁻¹	
$K_{2,2}$	$1.129 \times 10^8 e^{\left(\frac{-36648.7}{RT}\right)}$	Kmol bar ⁻¹ kgcat ⁻¹ h ⁻¹	
ρ_s	$\rho_s = 2337.9$	kg/m ³	Deken et al (1980)
ρ_B	1402.74	kg/m ³	$\epsilon = 0.4, assumed$

Steam reforming is carried out in a multi-tubular reactor and nickel is used commonly as a catalyst. The temperature has an important role on the equilibrium composition, and higher temperatures favor CH₄ conversion due to the endothermic nature of the reforming reactions. At elevated temperatures, the equilibrium shifts to produce more hydrogen and carbon monoxide, facilitating the breakdown of methane (CH₄) into its constituent products in processes such as steam reforming or dry reforming.

2.2.2.3 DME synthesis section

DME synthesis from synthesis gas (syngas: H₂+CO gas) has been developed for the past years. In the process of direct DME synthesis from natural gas, the natural gas will be converted to syngas of H₂/CO=1 with by product CO₂. Then the total process follows overall reaction (2.18), and eventually natural gas (methane) is converted into DME and water (Figure 9).

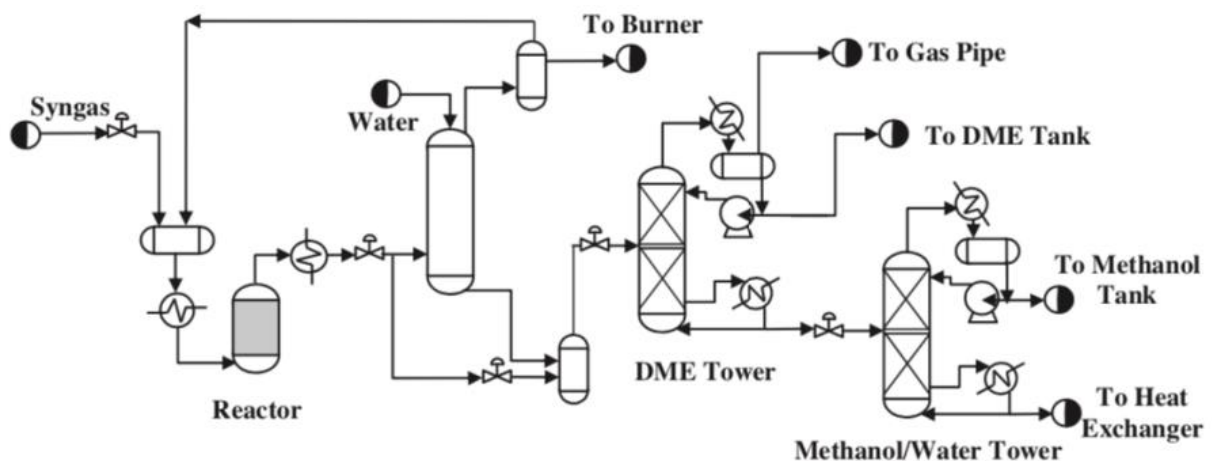
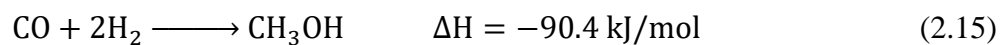


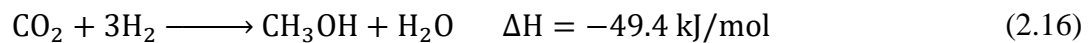
Figure 9: Direct DME production scheme (Fortin et al., 2020)

In this synthesis, H₂, CO and CO₂ are used to produce dimethyl ether in four reactions; three of them are depicted below, and the fourth one is the reaction in Equation 1 (methanol dehydration):

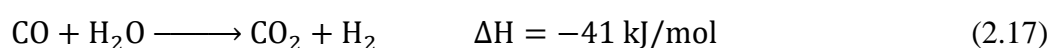
1. Methanol synthesis from CO



2. Methanol synthesis from CO₂



3. Water gas shift reaction (WGS)



According to Fortin et al (2020), the overall equation can be written as following, the first taking into account the WGS (Equation 2.17) reaction and the second without it:



Due to the high exothermic nature of this reactions of 2.18 and 2.19, temperature control is required. When the ratio of H_2 to CO equals the stoichiometric value, the maximum equilibrium conversion for each equation is obtained. The primary by product of this process is CO_2 . In order to recover CO and H_2 , it will therefore be utilized again in the methane reforming unit.



Banivaheb et al. (2022) provides, a comprehensive review of the state-of-the-art of kinetics models from Semi-Mechanistic, Data-Based and Hybrid Modeling Approaches. For an in-depth modelling of the kinetics of DME synthesis,

For the purposes of this research, a lumped model following Langmuir-Hinshelwood kinetics has been chosen to model the direct production of DME in Aspen HYSYS. Nie et al. (2005), proposed an intrinsic kinetics model of DME synthesis from syngas over a commercial by functional catalyst ($\text{CuO}/\text{ZnO}/\text{Al}_2\text{O}_3$) under a tubular integral reactor at 3–7 MPa and 220–260°C. The three reactions (equations 2.15 and 2.16) including methanol synthesis (equation 2.17) from CO and H_2 , CO_2 and H_2 , and methanol dehydration were chosen as the independent reactions.

The Langmuir-Hinshelwood model is presented for dimethyl ether synthesis; the parameters of the model were obtained by using simplex method combined with genetic algorithm (Nie et al., 2005). The model is reliable according to statistical analysis and residual error analysis. The model is as follows:

$$r_{\text{CO}} = \frac{k_1 f_{\text{CO}} f_{\text{H}_2}^2 (1 - \beta_1)}{(1 + K_{\text{CO}} f_{\text{CO}} + K_{\text{CO}_2} f_{\text{CO}_2} + K_{\text{H}_2} f_{\text{H}_2})^3} \quad (2.21)$$

$$r_{\text{CO}_2} = \frac{k_2 f_{\text{CO}_2} f_{\text{H}_2}^3 (1 - \beta_2)}{(1 + K_{\text{CO}} f_{\text{CO}} + K_{\text{CO}_2} f_{\text{CO}_2} + K_{\text{H}_2} f_{\text{H}_2})^4} \quad (2.22)$$

$$r_{DME} = \frac{k_3 f_{CH_3OH} (1 - \beta_3)}{(1 + \sqrt{K_{CH_3OH} f_{CH_3OH}})^2} \quad (2.23)$$

$$\beta_1 = \frac{f_{CH_3OH}}{K_{f1} f_{CO} f_{H_2}^2} \quad (2.24)$$

$$\beta_1 = \frac{f_{CH_3OH} f_{H_2O}}{K_{f2} f_{CO_2} f_{H_2}^3} \quad (2.25)$$

$$\beta_1 = \frac{f_{DME} f_{H_2O}}{K_{f3} f_{CH_3OH} f_{H_2}^2} \quad (2.26)$$

Where f_i is the fugacity of the reacting species and K_{fi} is the equilibrium constants of the reactions, K_i is the adsorption constants of specie i.

The model parameters are depicted in Table 3 as per data presented by Nie et al. (2005).

Table 3: DME kinetic model parameters.

Parameter	Expressions	Source
k_1	$k_1 = 7.380 \times 10^3 e^{\left(-\frac{54307}{RT}\right)}$	Nie et al. (2005)
k_2	$k_2 = 5.059 \times 10^3 e^{\left(-\frac{67515}{RT}\right)}$	Nie et al. (2005)
k_3	$k_3 = 1.062 \times 10^3 e^{\left(\frac{43473}{RT}\right)}$	Nie et al. (2005)
K_{CO}	$K_{CO} = 3.934 \times 10^{-6} e^{\left(\frac{37373}{RT}\right)}$	Nie et al. (2005)
K_{CO_2}	$K_{CO_2} = 1.858 \times 10^{-6} e^{\left(\frac{53795}{RT}\right)}$	Nie et al. (2005)
K_{H_2}	$K_{H_2} = 0.6716 \times 10^{-6} e^{\left(-\frac{6476}{RT}\right)}$	Nie et al. (2005)
K_{CH_3OH}	$K_{CH_3OH} = 3.480 \times 10^{-6} e^{\left(-\frac{54689}{RT}\right)}$	Nie et al. (2005)

Karagoz (2014) summarizes the typical operational conditions that DME direct synthesis is employed at industrial scale. The said conditions are presented in Table 4.

Table 4: DME synthesis operational conditions.

Syngas to DME	Conditions
Temperature (°C)	240 - 280
Pressure (bar)	30 - 70
H ₂ / CO ratio	0.7 - 1
Catalysts	Cu–ZnO–Al ₂ O ₃ /HZSM-5
Reactor types	Fluidized-Bed, slurry phase, fixed bed reactors

The methanol synthesis and water-gas shift reaction are catalyzed by Cu–ZnO– Al₂O₃. On the other hand, the methanol dehydration reaction is catalyzed by an acidic catalyst: HZSM-5 (Karagoz, 2014). Aguayo et al. (2007), observed that the stoichiometry of reaction 2 (syngas) corresponds to that of methane and heavier hydrocarbons formation. Thus, runs carried out by feeding methanol show that the presence of hydrocarbons is insignificant in the whole range of operating conditions. This result shows that, due to its weak acid sites, γ -Al₂O₃ is a suitable acid function for avoiding the transformation of methanol and DME (more reactive in these processes) into C₂-C₄ olefins or into heavier hydrocarbons.

Fluidized-bed, slurry phase, and fixed bed reactors are used in direct DME production. The slurry phase reactor was initially suggested for this purpose by Air Products and Chemicals in 1991. Subsequently, both fixed-bed and fluidized-bed reactors were proposed as optimal choices. Among these reactor types, the fluidized-bed reactor exhibits lower gas-solid mass transfer resistance compared to slurry-phase and fixed-bed reactors. Given that the DME reaction is highly exothermic, effective heat removal and temperature control are crucial in the reactor operation. The fluidized-bed reactor stands out for its excellent temperature control, facilitated by successful mixing of catalyst particles within the bed (Karagoz, 2014).

2.2.2.4 Separation and purification section

The core concept outlined in this section is to extract CO₂ from the reformer and its subsequent recycling back into the process. Three distinct points within the system facilitate the recycling of CO₂. The first source originates from the acid gas removal unit, the second is obtained post-reforming, and the third arises from the DME reactor. These three CO₂ streams are merged within the system and directed to the reformer, where they participate in the reaction with CH₄ to generate syngas.

Absorption, adsorption, cryogenic, and membrane systems represent the typical technologies utilized for CO₂ separation. The choice of technology relies on various factors such as the CO₂ concentration in the feed, feed conditions like pressure and temperature, desired product purity, and the intended use of the product. Each technology has its own set of advantages and disadvantages. Absorption offers benefits like sorbent recycling and independence from constant operator intervention. However, it can be susceptible to issues such as carbon steel corrosion caused by oxygen and solvent degradation due to NO_x and SO_x. Adsorption, on the other hand, boasts advantages like sorbent recycling and operational flexibility. Nonetheless, it may struggle with high CO₂ concentrations, and smaller gases can be inadvertently adsorbed. Cryogenic technology, which operates at atmospheric pressure and doesn't require absorbents, provides another option. Nevertheless, it necessitates multiple steps to eliminate water, thereby escalating process costs (Brunetti et al., 2010).

Membrane systems emerge as a promising alternative to conventional separation methods, particularly suited for streams with CO₂ concentrations exceeding 15%, typically found in steel

production plants. These systems operate without moving components, emphasizing modularity, and offer rapid responses to fluctuations in conditions (Brunetti et al., 2010).

Another concern involves separating unreacted syngas from the reactor output. The unreacted syngas stream splits into two streams: one can be directed towards fuel production and the other recycled back into the DME reactor. The mixture comprising DME, methanol, and water undergoes distillation in the initial distillation column to isolate DME. In the second distillation column, the distilled methanol is recycled back to the DME reactor for further reaction. Figure 10 illustrates the direct synthesis pathway.

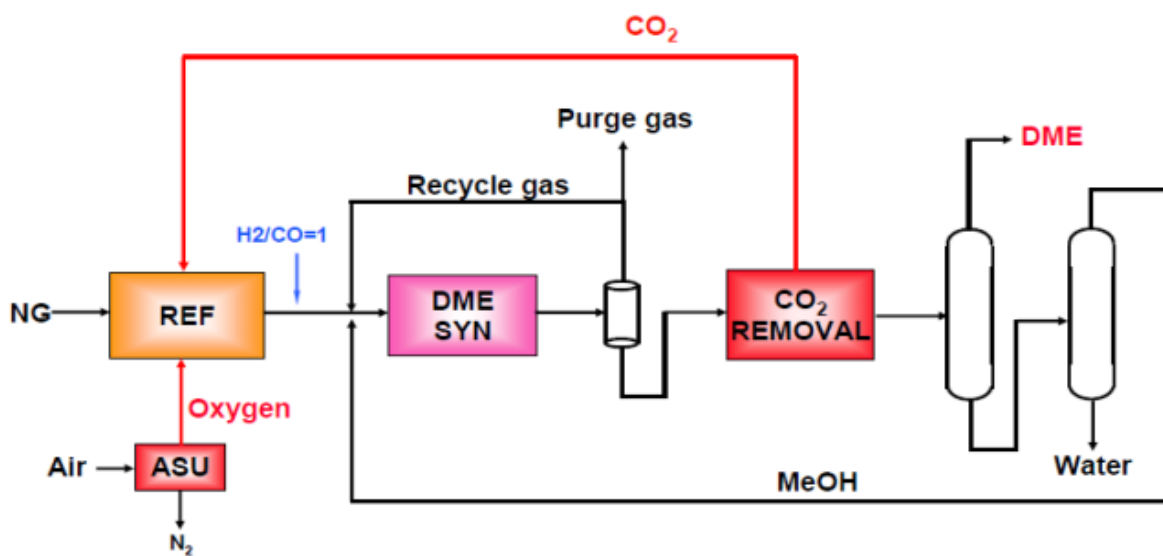


Figure 10: DME synthesis and purification process scheme.

2.3 USES OF DIMETHYL ETHER

Dimethyl ether (DME), is an affordable and environmentally friendly alternative fuel. DME shares many of the same characteristics as LPG. It is a clean, simple-to-handle fuel that may be utilized in a variety of applications, including transportation, power generation, home heating and cooking, and more (Ogawa et al., 2004). Figure 11 represents the common feedstocks and uses of DME.

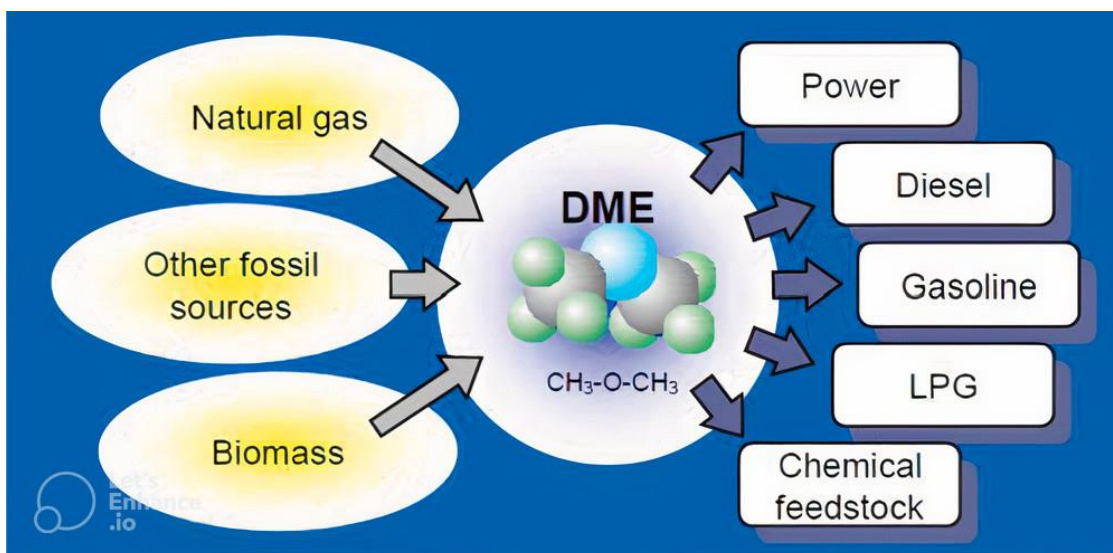


Figure 11: DME feedstocks and common applications (Gogate, 2018)

Liquefied petroleum gas (LPG) mixture has been the most popular use in recent years. LPG shortage is a threat, in fact. Moreover, DME is a viable LPG alternative due to its high cetane number, low toxicity, and good flammability. Additionally, methanol, biomass, and syngas are among the several raw materials that may be used to generate DME, supporting both market expansion and increased output. LPG is combined with DME and utilized in China's homes and industries for many purposes, including cooking. Dimethyl ether is an additional green refrigerant option. Indeed, its global warming potential is substantially lower than that of chlorofluorocarbons and it has minimal ozone depletion potential (Fortin et al., 2020).

Additionally, DME finds significant usage as a feedstock in the synthesis of other compounds, such as light olefins, methyl acetate, and dimethyl sulphate. Because of the Monsanto method, DME may also be carbonylated into acetic acid (Azizi et al., 2014).

2.4 LIQUEFIED NATURAL GAS PRODUCTION PROCESS

There are primarily two ways to transport natural gas: gaseous or liquefied natural gas (LNG). At the moment, pipelines are widely used to carry natural gas in gaseous form. For short- to medium-length overland transit distances, pipelines are appropriate. Due to the lack of a capital-intensive liquefaction facility and regasification terminal, pipelines are less expensive at these distances than LNG chains. In contrast to LNG, which typically uses around 25% of the energy provided, gas is typically delivered by pipeline at a cost of 10-15% of the energy delivered. Pipeline transportation produces fewer greenhouse gas emissions (GHG) than LNG. But as the distance of transportation increases, the pipeline's benefits diminish. Pipes that exceed 4800 km in length on land and over 1600 km in length offshore. Energy consumed and GHG emissions are equal for onshore pipelines and LNG with distances of 13,000 km and 7500 km, respectively (Mokhatab et al., 2015).

For alternative transport, natural gas is condensed by cooling it down to $-162\text{ }^{\circ}\text{C}$ at atmospheric pressure, thereby reducing its volume by a factor of 600. Produced LNG is transported cryogenically by truck, train or vessel. One advantage of LNG is that one liquefaction plant can serve several regasification plants and vice-versa. Furthermore, LNG can easily adjust its supply capacity and destination, making it more adaptable than pipeline gas (Mokhatab et al., 2015). Another advantage of LNG is that small-scale LNG and offshore LNG allow the exploitation of remote small gas resources and offshore gas reserves, for which it is not economical to build a pipeline (Yuan et al., 2014).

The intricate supply chain of liquefied natural gas (LNG) facilitates the transportation of natural gas to consumers worldwide. In summary, LNG value chain encompasses various stages from production to consumer delivery, as depicted in Figure 12. Beginning with the exploration and extraction of natural gas resources, often in remote locations both onshore and offshore, the process involves drilling wells to bring the gas to the surface for treatment. The extracted gas contains non-hydrocarbon elements such as hydrogen sulfide, nitrogen, carbon dioxide, and water, which are removed during the treatment phase as depicted in Figure 12. Subsequently, the purified natural gas undergoes liquefaction and refrigeration at specialized facilities. The conversion of NG into LNG is, notably costly and energy-intensive process. Following liquefaction, the LNG is stored in insulated tanks prior to shipment. Specially designed vessels

transport the LNG at extremely low temperatures to receiving and regasification facilities, where it is converted back into natural gas before final delivery to consumers (Lee et al., 2018).

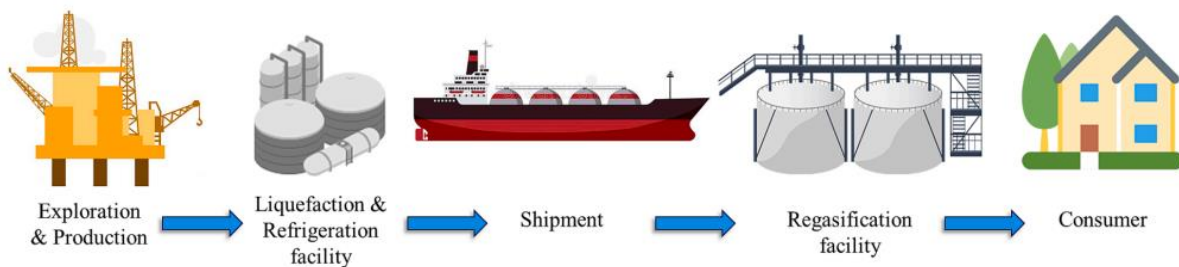


Figure 12: LNG supply chain (Bassioni & Klein, 2023)

The liquefaction stage stands out as the most formidable aspect of the LNG supply chain, consuming a substantial 28% of the total process cost. Before liquefaction can occur, the gas must undergo through cleaning and drying. This involves the removal of non-hydrocarbon residues like carbon dioxide (CO₂) and hydrogen sulfide (H₂S).

Additionally, the gas is cooled to facilitate water condensation, with a subsequent dehydration procedure used to eliminate any remaining water vapor. Preceding the liquefaction step, a purification procedure is necessary to ensure the absence of liquid hydrocarbons. The Natural Gas Liquid (NGL) recovery unit then receives the treated gas, aiming to produce a lean gas suitable for liquefaction by extracting C₂₊ and C₃₊ hydrocarbons. This lean gas initiates the liquefaction process, renowned for its high cost, energy demand, and complexity within LNG production facilities. The process relies on refrigeration cycles, involving a sequence of expansion and compression cycles to dissipate heat. Two main methods are employed: a closed-cycle process utilizing a heat exchanger with a separate fluid circulation, or an open-cycle process where the refrigerant is part of the natural gas supply. Achieving the ultra-low temperature required for liquefaction (-162°C) necessitates the use of refrigerant compressors, possibly multiple units. This temperature is attained through three distinct zones: precooling, liquefaction, and sub cooling (Bassioni & Klein, 2023).

2.4.1 LIQUEFACTION PRINCIPLES

LNG technologies are based on refrigeration cycles. The refrigeration process consists of four primary stages: first, the refrigerant is compressed to generate a high-pressure, hot stream (compression by a compressor); second, heat is released from the compressed refrigerant (occurring in the condenser or cooler and heat exchanger); third, the compressed refrigerant expands to form a low-pressure, cold stream (via a valve or expander); and finally, heat is absorbed by the cold refrigerant (in a heat exchanger). It's in this final stage that the cooling required for the natural gas occurs. By cyclically repeating these four steps, continuous cooling of the natural gas can be achieved (Zhang et al., 2020).

LNG technologies can be categorized into three main types: cascade technology (Cascade), mixed refrigerant technology (MR), and expander-based technology. The next sections will focus on giving a brief description of the liquefaction technologies.

2.4.2 CASCADE LIQUEFACTION PROCESS

Every refrigeration cycle in the cascade liquefaction process may be independently regulated, making it a versatile process. Cascade processes come in two varieties: pure refrigerant cascade process and a cascade process using mixed refrigerant (MR).

In the pure refrigerant cascade process: propane, ethylene, and methane are used as heat exchange fluids in the pure refrigerant process. The propane cycle is contributing as precooling of NG feed for ethylene condensation. The ethylene condenses the NG feed in addition to methane in the final cycle. The methane cycle then sub cools the LNG. The overall schematic diagram is shown in Figure 13. The design of an LNG carrier assures coolness, nevertheless it is not perfectly isolated against warming. Heat may slowly affect the tanks resulting LNG to evaporate to produce boil-off gas (BOG). BOG increases the tank pressure due to larger gas volume. The advantage of this process is the low surface area required for the heat exchanger, with low technical risk. However, the disadvantages are the need for high capital investment and insufficient adaptation to the variation in the NG composition (Bassioni & Klein, 2023).

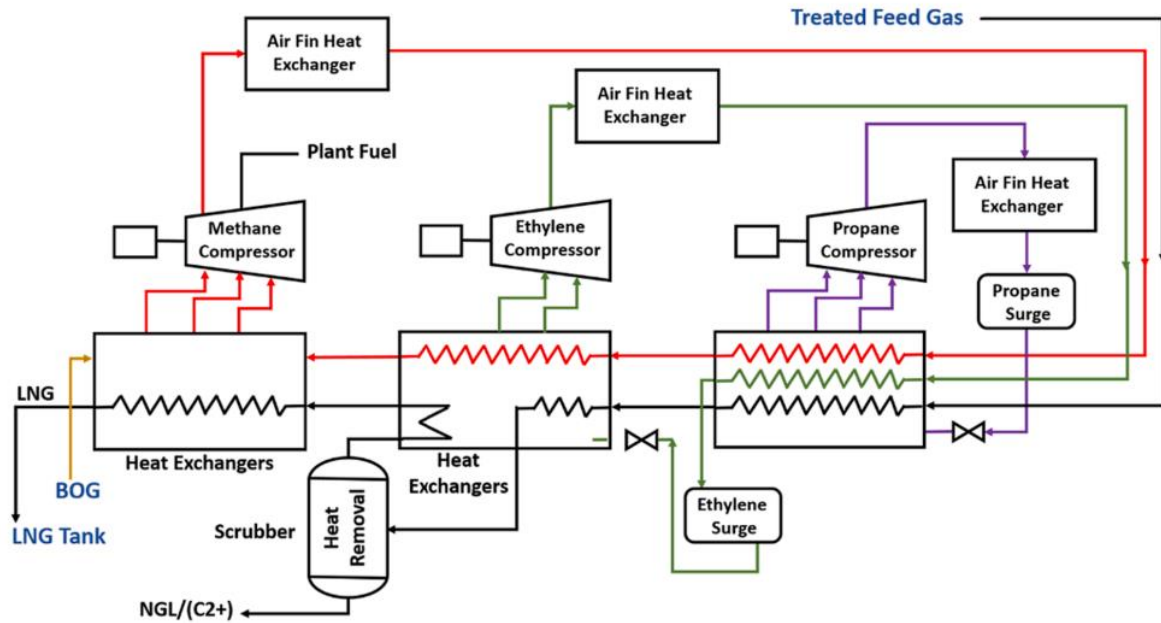


Figure 13: Pure refrigerant cascade process (Bassioni & Klein, 2023)

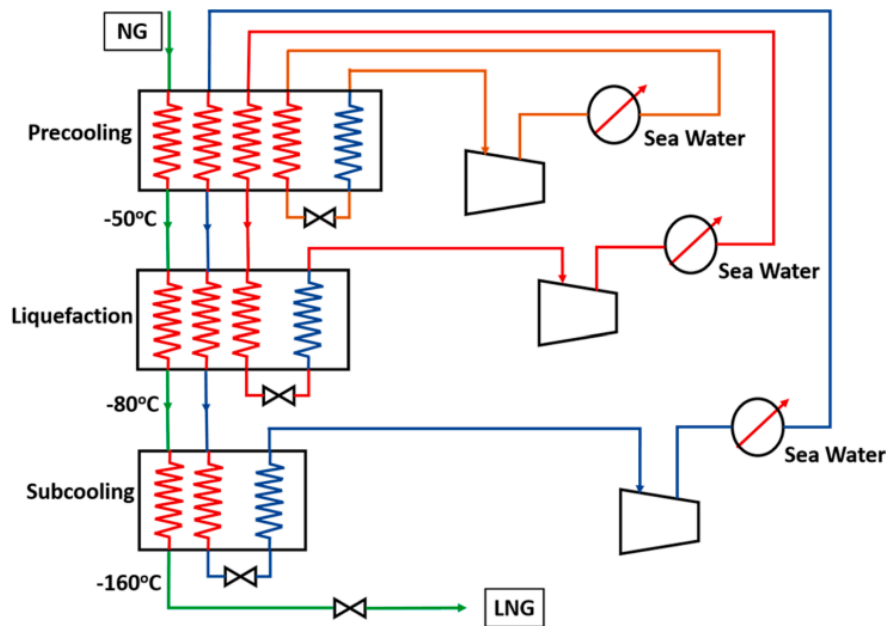


Figure 14: Mixed refrigerant (MR) cascade process (Bassioni & Klein, 2023)

In the Mixed refrigerant (MR) cascade process, the process utilizes mixed refrigerants all together in the three cooling zones. The process closely matches the cooling curve in the heat exchanger, as compared to the pure refrigerant cascade process, which provides higher

efficiency of the used energy. The overall MR cascade process schematic diagram is shown in above Figure 14. The advantages of the MR cascade refrigerant process are having close operation temperature to the NG cooling curve, and the ability to adjust the refrigerant composition according to the NG composition. The disadvantage is that the process shows a slower dynamic behavior than the mixture of refrigerant needs to be adjusted depending on the NG feed composition (Bassioni & Klein, 2023).

2.4.3 MIXED REFRIGERANT LIQUEFACTION PROCESSES

Mixed refrigerant systems employ a combination of refrigerants in one or multiple cycles to convert natural gas (NG) into liquefied natural gas (LNG). These systems typically use refrigerant fluids found in cascade processes (like propane, ethylene, and methane). However, some methods add nitrogen to the mix, creating a binary mixture. This addition raises the refrigerant's bubble-point near the sub-cooling point, enhancing efficiency and reducing operational pressure. Various types of mixed refrigerant processes exist, including the mixed refrigerant cascade process, single mixed refrigerant (SMR) process, and dual mixed refrigerant (DMR) process (Jensen & Skogestad, 2006).

2.4.3.1 Single Mixed Refrigerant (SMR)

The SMR process comprises several stages: compression, cooling (using either air or water), expansion via a valve, and a cryogenic multisystem exchanger for both cooling and evaporation. Initially, the natural gas (NG) feed enters the heat exchanger at high pressure and ambient temperature, where it exchanges heat with a mixed refrigerant (MR) whose composition depends on various factors including the NG feed's composition, pressure, ambient temperature, and liquefaction plant pressure. Subsequently, the NG is transformed into subcooled LNG and immediately subjected to slightly higher than atmospheric pressure by the expansion valve. Conversely, the MR stream undergoes compression via multiple compressors and is then evaporated within the heat exchanger, where pressure is reduced by the expansion valve (Bassioni & Klein, 2023).

Notably, the SMR process is suitable primarily for small to medium-sized liquefaction plants due to its comparatively lower energy efficiency than alternative processes. The schematic diagram of the SMR process is depicted in Figure 15.

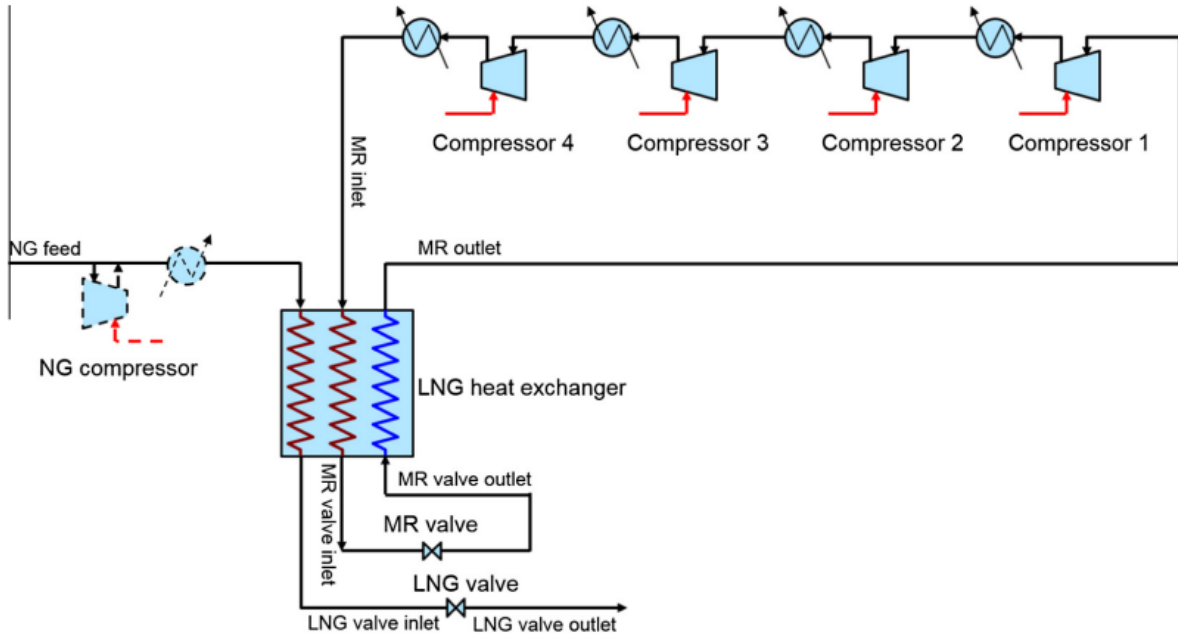


Figure 15: Single Mixed Refrigerant Diagram.

2.4.3.2 Dual Mixed Refrigerant (DMR)

This method involves liquefying the natural gas (NG) feed through two distinct refrigerant stages. Initially, a heavier mixed refrigerant (MR) is employed to precool the NG feed, followed by a second step utilizing a lighter MR where the cooled NG is condensed within the heat exchanger. The heat exchanger's size is halved compared to the SMR process since the cooling cycle is divided into two stages. The schematic diagram of the DMR process is illustrated in Figure 16. The most commonly utilized form of DMR is the propane-precooled mixed refrigerant process, known as C3-MR (Zhang et al., 2020; Bassioni & Klein, 2023).

In this process, pure propane (C3) is used for precooling, while the liquefaction and sub cooling stages utilize the MR stream. This method is predominant due to its high energy efficiency, resulting from close alignment between the NG cooling curve and the boiling curve of the refrigerant. However, certain challenges are associated with this process, including a significant requirement for propane inventory and a higher level of design complexity (Zhang et al., 2020; Bassioni & Klein, 2023). The C3-MR process is licensed by Air Products and Chemicals, Inc. (APCI), with its schematic diagram depicted in Figure 17.

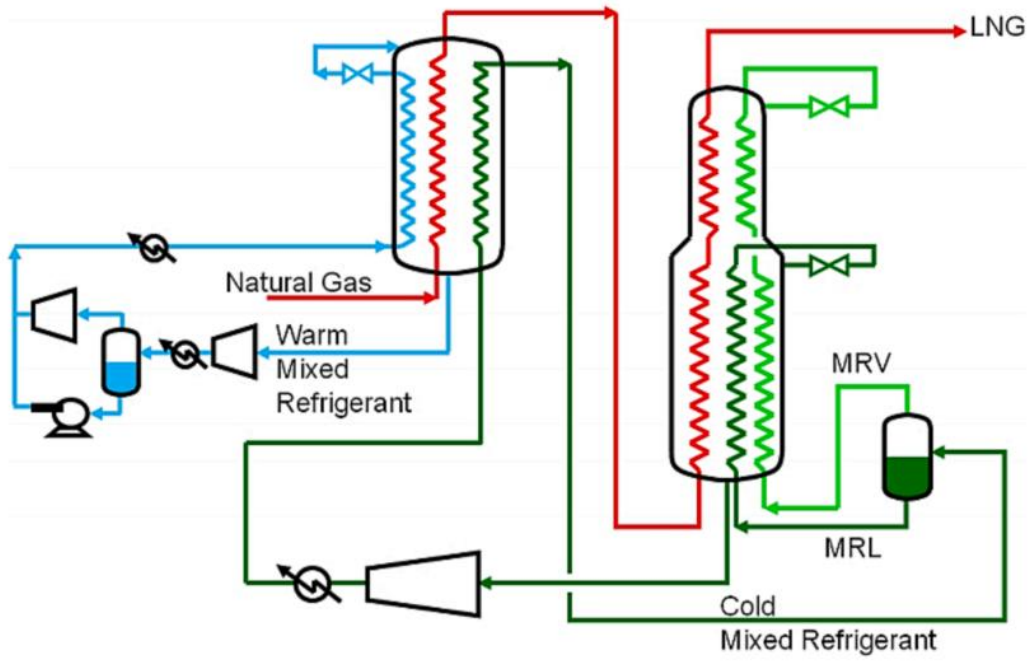


Figure 16: DMR process diagram (Bassioni & Klein, 2023)

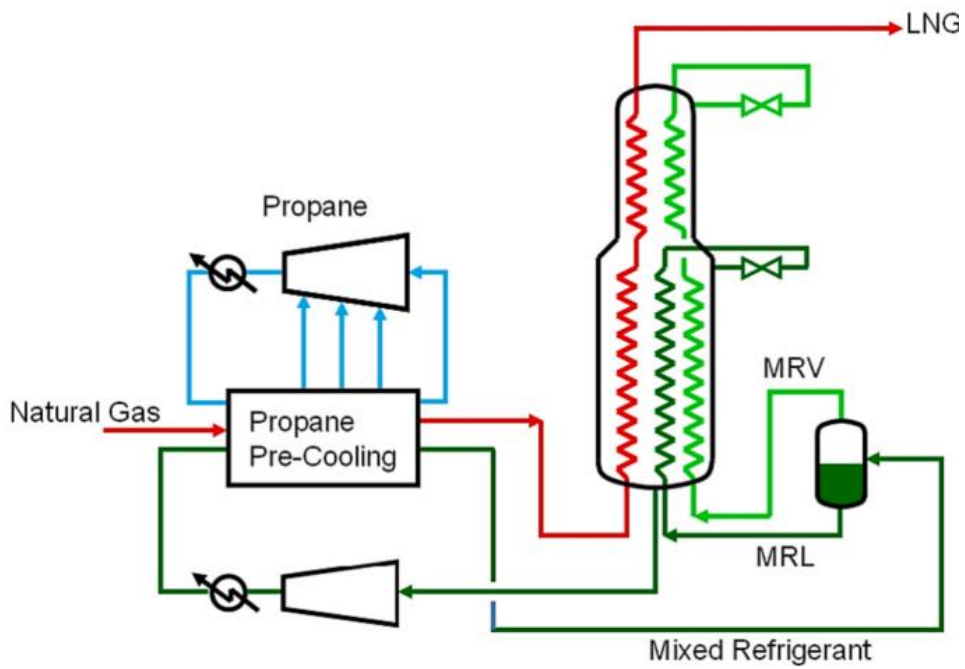


Figure 17: C3-MR process diagram (Bassioni & Klein, 2023)

2.4.4 EXPANSION-BASED PROCESSES

This method functions by employing a turbo-expander to produce the refrigeration necessary for the liquefaction process. Utilizing compression and expansion cycles facilitated by the turbo-expander, refrigeration is generated from a fluid. Various configurations exist, including single, dual, or multiple turbo-expanders. In the case of larger expanders, the mechanical power produced can be utilized to operate either an electric generator or a compressor. Methane or nitrogen serve as the refrigerants, maintaining their gaseous state throughout the refrigeration cycle. As the refrigerant consists of a single component, there is no need for composition adjustments, thereby simplifying operational requirements. Furthermore, the process displays reduced sensitivity to changes in the composition of the natural gas feed, as the heat exchanger can function effectively across a broad temperature range. Consequently, the primary advantage of this method lies in its operational stability. However, its efficiency is lower when compared to cascade or mixed refrigerant processes (Bassioni & Klein, 2023). The nitrogen (N_2) expander-based approach (Figure 18) is regarded as a promising solution for offshore applications.

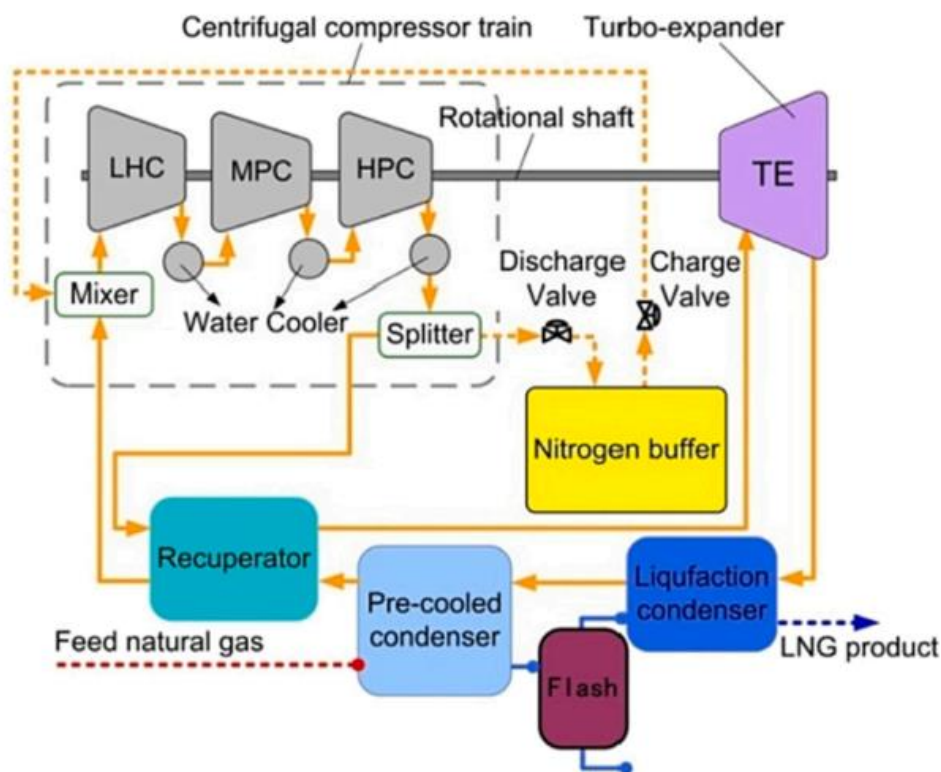


Figure 18: Typical N_2 expansion process diagram (Bassioni & Klein, 2023)

2.4.5 COMPARISON OF THE LIQUEFACTION TECHNOLOGIES

The variances among the technologies primarily stem from their inherent complexities: Cascade employs three separate cycles, MR utilizes a single cycle with a mixed refrigerant, and expander operates with a single cycle using pure refrigerant. The assessment of the criteria for the three LNG technologies relies on a comparative analysis. The energy consumption during liquefaction is closely tied to the cooling curve of the process (Zhang et al., 2020). As depicted in Fig. 19.

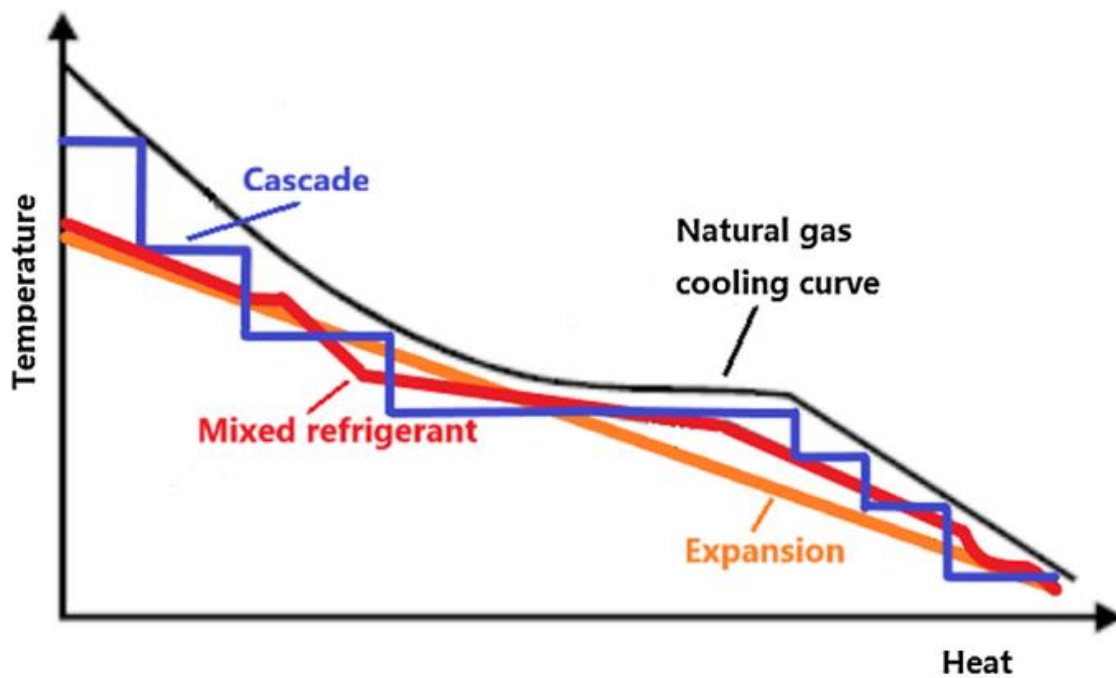


Figure 19: LNG cooling curve of Cascade, MR and EXP (Zhang et al., 2020)

Cascade exhibits multiple cooling temperature levels due to its utilization of multiple refrigerants, enabling minimal temperature differentials between the hot and cold sides in the heat exchangers. MR, by employing a refrigerant composed of a carefully selected mixture of hydrocarbons, can replicate the natural gas cooling curve with even smaller temperature differentials compared to Cascade, albeit at the expense of requiring a larger heat exchange surface area.

In contrast, the pure refrigerant used in the expander technology maintains a gaseous state throughout the process, resulting in a consistent specific-heat value for the cooling curve. However, the expander technology experiences a relatively large temperature differential between the refrigerant and natural gas, particularly at the high-temperature end, leading to higher energy consumption.

The pros and cons of the three LNG technologies are outlined in Table 5, adapted from Lim et al. (2012) and Zhang et al. (2020).

Table 5: LNG technologies comparison.

Criteria	Cascade	MR	EXP
Application	Onshore large-scale	Onshore large-scale, small-scale and offshore	Onshore small-scale and offshore
Energy efficiency	High	Medium to high	Low
Equipment count	High	Low to medium	Low
Heat-transfer surface area	Medium	High	Low
Simplicity of operation	Low	Low to medium	High
Ease of start-up and line-up	Medium	Low	High
Adaptability of feed-gas compositions	High	Medium	High
Sensitivity to ship motion	High	Medium to high	Low
‘Space requirement	High	Medium	Low
Hydrocarbon-refrigerant storage	High	Medium to high	‘None
Capital costs	High	Low to medium	Low

2.5 LIQUEFIED NATURAL GAS STORAGE, TRANSPORTATION AND BOIL-OFF GAS

The optimal method for transporting natural gas is via pipelines; however, the most cost-effective and efficient mean for long-distance transportation of natural gas resources across regions within the framework of globalization has evolved to be the transportation of liquefied natural gas (LNG) via ships. An LNG receiving terminal serves the purpose of storing LNG and subsequently vaporizing and transferring it to the downstream gas terminal through an

evaporation facility, which has significance in the overall LNG industry process chain. Figure 20 illustrates the operation process in the LNG receiving terminal, which consists of pumps, compressors, tank, recondenser and vaporizer (Wu et al., 2019).

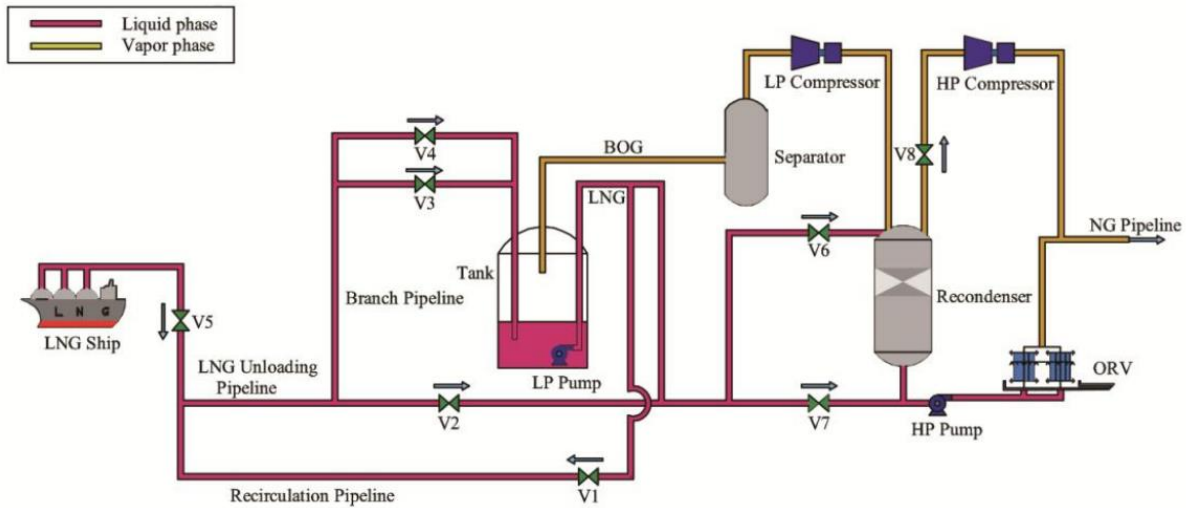


Figure 20: LNG receiving terminal (Wu et al., 2019)

One of the primary challenges encountered in the LNG sector involves the emergence of Boil-off Gas (BOG) during both storage and loading processes, namely Tankage Boil-off Gas (TBOG) and Jetty Boil-off Gas (JBOG). BOG, originating from LNG, is produced as a result of LNG depressurization, heat infiltration through tanks and pipes, and additional heat introduced to LNG from various operational procedures like LNG pumping (Bouabidi et al., 2021). The volume of BOG experiences rapid increment and significant fluctuations, particularly during the unloading phase, leading to potential physical harm to equipment and heightened power consumption of compressors (Park et al., 2010). Hence, it holds practical importance for the daily operation of the LNG receiving terminal to precisely optimize the unloading procedure in order to minimize power consumption (Bouabidi et al., 2021, (Park et al., 2010).

During routine operations at the LNG receiving terminal, the generation of BOG due to temperature discrepancies along the pipe can result in deformations caused by thermal expansion or contraction, potentially leading to stress on the pipeline and equipment, which may affect the integrity and safety of the system. The temperature variations occur due to the formation of a vapor space atop the pipe. This phenomenon, known as geysering, propels the two-phase flow into the inlet nozzle of the storage tank, subjecting the tank to shock and

vibration, potentially causing significant equipment damage depending on the severity. Therefore, in LNG receiving terminals, a recirculation operation is done to reduce the inflow of BOG into the storage tank by keeping the unloading pipes in a cryogenic condition (Jung & Corporation, 2000).

Therefore, it makes it clear that knowledge of the amount of BOG created during LNG shipping and piping is of importance evaluation. Since this project, looks at both LNG and DME as potential energy carriers, the BOG analysis conducted at same conditions for both commodities. Here, the author considers that the same infrastructure used to store, convey, and transport LNG can be used to convey, transport and store DME.

2.5.1 BOIL-OFF RATE

This represents the speed at which LNG boils off into vapor when subjected to changes in temperature. It denotes the proportion of liquid evaporating from a cargo, storage tank, or process line due to heat leakage. Usually, the boil-off rate is expressed as a percentage of the total liquid volume per unit time (Ezeh et al., 2019). This rate can be determined using the following formula:

$$\text{BOR} = V_{\text{BOG}} \times \frac{24}{V_{\text{LNG}} \cdot \rho} \quad (2.27)$$

$$\text{BOR} = Q \times \frac{3600 \cdot 24}{\Delta H \cdot V_{\text{LNG}} \cdot \rho} \times 100 \quad (2.28)$$

Where:

BOR= boil of rate in % /day; V_{BOG} is volume of BOG in m^3/s ; V_{LNG} is volume of LNG in cargo tanks in m^3 ; ρ density of LNG in kg/m^3 ; Q heat exchange in W, (KJ/s); ΔH latent heat of vaporization in J/kg.

Typical BOR caused by heat ingress for newer LNG tankers ranges from 0.10% to 0.15% for laden (loaded) voyage and from 0.06% to 0.10% for ballast voyage (Hasan et al., 2009).

The quantity of BOG depends on the design and operating conditions of storage tanks and a ship's cargo tanks. The holding phase, as described by Sedlaczek (2008) denotes the duration between the loading and unloading of LNG tankers. At loading and receiving terminals, LNG

is held within cryogenic storage tanks under standard operating pressure, typically ranging from 0 to 0.15 bar below atmospheric pressure. During this holding phase, two primary sources contribute to the generation of boil-off gas: heat infiltration into the storage and pipes from the surroundings, and variations in ambient (barometric) pressure. Most of BOG is generated during transportation of LNG by ships (Dobrota et al., 2013).

Heat ingress from the surroundings means that BOG is generated continuously in the tanks. In order to reduce boil-off, storage tanks have multi-layered insulation that minimizes heat leakage. The driving factor behind heat infiltration into an LNG tank is the contrast between the external temperature and the temperature within the tank. Owing to substantial temperature differentials between the contents and the surroundings, heat can permeate into the LNG through the floor, walls, and roof of storage tanks (Figure 21) via three mechanisms: conduction, convection, and radiation (Dobrota et al., 2013).

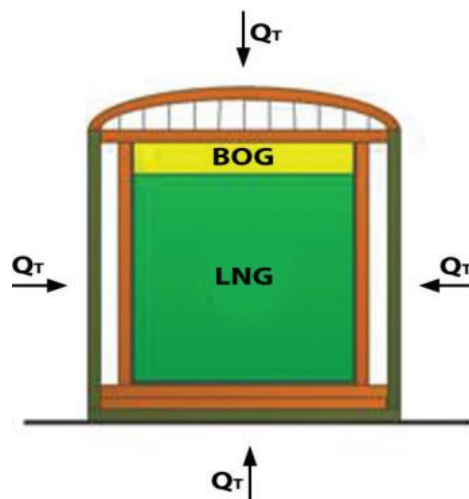


Figure 21: Heat ingress in LNG tank (Dobrota et al., 2013)

The loading/unloading mode is the period when an LNG tanker is moored to the jetty at loading and receiving terminals and connected to onshore storage tanks with loading/unloading arms and insulated pipelines. During the unloading of an LNG tanker, differences in operating pressures between the ships and the terminal's storage tanks can also influence the quantity of BOG. The LNG cargo attains an equilibrium temperature dependent on the cargo tank pressure (Dobrota et al., 2013).

2.5.2 RECOVERY OF BOIL-OFF GAS

BOG produced during holding mode in storage tanks is usually called tankage BOG (Hasan et al., 2009). When heat is introduced to LNG, the vapor pressure within the tank rises. To ensure that the tank pressure remains within a safe range, tankage BOG needs to be extracted using compressors.

Typically, at loading terminals, BOG serves as fuel in the production process of the liquefaction plant. Conversely, at receiving terminals, it is either combusted or directed to the re-gasification plant through BOG compressors (Dobrota et al., 2013). Figure 22 serve as an example.

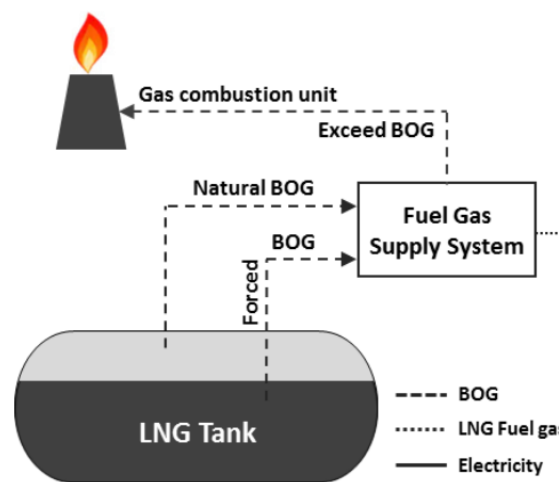


Figure 22: BOG Recovery system (Kim et al., 2019)

In their study, Kurle et al. (2015) examined the C3-MR liquefaction process and suggested various approaches for reusing BOG, including utilizing it as a fuel gas, recycling it as a feed gas, liquefying it onshore, and liquefying it at the berth. They determined that a temperature of approximately 166°C represents the optimal point where total costs are minimized. This temperature minimizes the amount of BOG while maximizing recovery. Additionally, Kurle et al. (2015) concluded that using BOG as fuel gas was the most energy-efficient strategy among those considered. However, while these approaches offer cost-effective solutions, they neglect environmental considerations. Recycling strategies like these lead to nitrogen accumulation in the system, which in turn increases NO_x and CO₂ emissions, gradually raising operational costs.

For further reading regarding BOG recovery, the author recommends the reader to look at the paper from Bouabidi et al. (2021), which provides a broader overview of the state-of-the-art of the recovery technologies of the BOG.

CHAPTER III

3 RESEARCH METHODS

This study employs a simulation-based approach utilizing Aspen HYSYS. Aspen HYSYS is, a comprehensive process simulation tool widely recognized for its capabilities in modeling complex chemical processes. The present research involves design and analyzing simulation models to represent the production pathways of Dimethyl Ether (DME) and Liquefied Natural Gas (LNG) derived from natural gas feedstock.

The simulation model for the standard DME and LNG production processes will be built entirely with Aspen HYSYS, where the mass, energy and momentum balance will be done according to the embedded equations. The thermodynamic package chosen to predict the fluids properties is Peng-Robinson Equation of State (PR-EOS) for the LNG production. A modified Redlich-Kwong-Soave EOS is used to predict DME properties (solubility and binary interactions) in the synthesis reactor.

The steady state simulation results will be used to compute, analyze and compare the energy intensities of the production processes of the two commodities, DME and LNG. For this purpose, Aspen Energy Analyser will be used to determine the energy intensities.

The data needed to conduct this study within the scope defined in research are:

1. Kinetics data for DME synthesis;
2. Composition of natural gas feedstock;
3. Typical operational conditions for both processes.

All the aforementioned data will all be obtained by reviewing the literature in articles and manuals that discuss issues related to the topic under the study. .

For the BOG calculation, each steady state flowsheet will be converted to dynamic simulation in order to calculate the increment of pressure with the storage vessels as over time and the energy carriers (LNG and DME) exchange heat with the environment. This pressure increase will be computed, analysed, and compared for the two commodities.

A sensitivity analysis will also be done by systematically varying input parameters within acceptable ranges to assess their impact on the overall process, including boil-off gas generation and energy intensity.

3.1 SIMULATION MODEL DEVELOPMENT

The following sections; aim at describing the methodology and parameters used to simulate the two production process (DME and LNG). The storage tanks of both processes that are simulated to estimate the BOG generation are described in the same sections, since both processes were simulated under similar conditions.

3.1.1 DIMETHYL ETHER PRODUCTION PROCESS

The DME production process can be divided into two subsections, where the first one is the syngas generation and the second one is the DME synthesis. In this research, the syngas production is carried out by combining a stream of natural gas at 8 bar and ambient temperature (25 °C), and saturated steam stream at 30 bar and 405 °C. Before starting the process, natural gas is first compressed to 30 bars; to meet the operating pressure of a typical steam methane reforming process, for the steady state simulation as depicted in Figure 23.

This mixture of hydrocarbons and steam (HC/S) is heated up to 500 °C and sent to a pre-reformer, where the heavy hydrocarbons molecules present in natural gas are converted into methane, to avoid carbon deposition on the reformer tubes (coking). The reaction in the pre-reformer is endothermic, thus the HC/S is again heated to 620 °C to enter the reforming reactor. Due to limitations of the simulator used, the autothermal reforming is simulated using two units: a fired heater to supply the heat need for reforming reaction followed by a multi-tubular plug flow reactor, representing the tubes of the reformer. The reforming reaction are simulated using the Xu and Froment (1989) kinetics as described in section 2.2.2.

Steam is generated by recovering heat from the reformer flue gas and pre-heated with the reformate leaving the reformer. After being cooled, the reformate passes through a flash tank to separate the condensate water. In sequence CO₂ (in Carbon Capture and Storage (CCS) unit simulated as component splitter) and non-converted methane (in Pressure Swing Adsorption (PSA) unit simulated as component splitter) are separated. This; yields a stream of syngas ready to undergo DME synthesis.

Syngas is heated up to 180 °C and in sequence fed to a Gibbs reactor for the formation of DME. The reactions products are sent to a distillation column to produce a DME rich stream in the top side of the column and a methanol rich stream on the bottom side of the column. The DME rich stream is then fed to a flash tank to strip out all the vapors from the liquid before it is sent to the storage tank.

For this flowsheet, the thermodynamics properties were estimated by the Soave-Redlich-Kwong Fluid Package, since there is a presence of polar compounds in the process. Operating conditions of each one of the streams depicted on Figure 23 is shown on Appendix A. Natural gas composition used in the simulation is depicted in Table 6.

Table 6: Natural gas composition

Component	Fraction
Methane	95.38%
Ethane	2.06%
Propane	0.87%
i-Butane	0.22%
n-Butane	0.25%
i-Pentane	0.82%
n-Pentane	0.04%
n-Hexane	0.02%
n-Heptane	0.02%
n-Octane	0.07%
n-Nonane	0.00%
n-Decane	0.02%
Oxygen	0.00%
Nitrogen	0.21%
H ₂ O	0.00%
CO	0.00%
CO ₂	0.01%

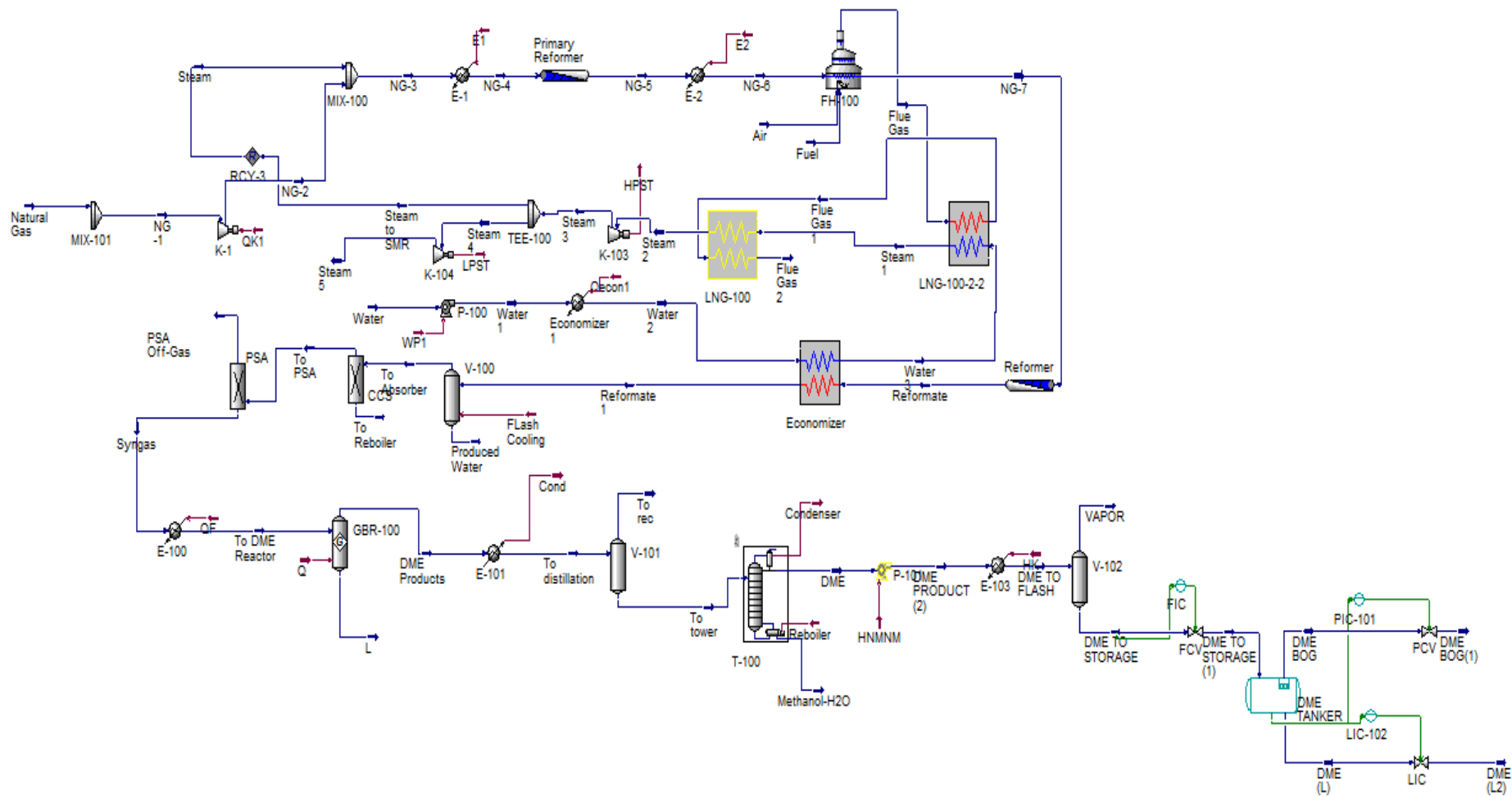


Figure 23: Dimethyl ether production and storage process flow diagram.

3.1.2 LIQUEFIED NATURAL GAS PRODUCTION PROCESS

The steady state flowsheet depicting the process can be seen in Figure 24. For this process the fluid package selected to predict the thermodynamic properties is Peng-Robinson, since the compounds are mainly nonpolar hydrocarbons (alkanes). The depicted circuit as well as the composition of the mixed refrigerant are based on the extensive work done by Helgestad (2009).

The initial phase involves cooling with propane. Natural gas is first pre-cooled to around -36°C using the propane cycle. It then passes through the main cryogenic heat exchanger (MCHE), where it is liquefied and further cooled to approximately -155°C by the mixed refrigerant cycle in the C3MR cycle. Typically, the natural gas entering the process is at a pressure of about 40 bar. To achieve the LNG product specification of around -160°C , the gas is expanded isenthalpically through a valve (Joule-Thompson effect).

The propane cycle also pre-cools the mixed refrigerant. Propane is compressed to 6 bar, allowing it to condense using cooling water. This means the pressure must be sufficient for propane to remain in the liquid phase at the cooling temperature. The liquid propane is then depressurized and vaporized through heat exchange with natural gas and mixed refrigerant. This process occurs in three stages, with the propane vapor returning to compression after each stage. The final heat exchangers in the propane cycle must superheat the propane to prevent liquid from entering the first compressor. After pre-cooling, the mixed refrigerant is partially condensed and sent to a high-pressure separator before entering the main cryogenic heat exchanger (MCHE's). The vapor and liquid mixed refrigerant streams travel through separate circuits in the MCHE-1, where they are cooled, liquefied, and sub-cooled through internal heat exchange with the natural gas. These sub-cooled refrigerant streams are then depressurized, lowering their temperature to cool specific areas of the MCHE-2. As the low-pressure refrigerant streams descend through the MCHE-2, they vaporize and superheat by cooling the natural gas and the mixed refrigerant streams. The superheated low-pressure mixed refrigerant is then recompressed and water-cooled to complete the cycle. This process produces high-pressure natural gas at approximately -155°C , which is then expanded to atmospheric pressure, resulting in LNG at 1 atm and -160°C .

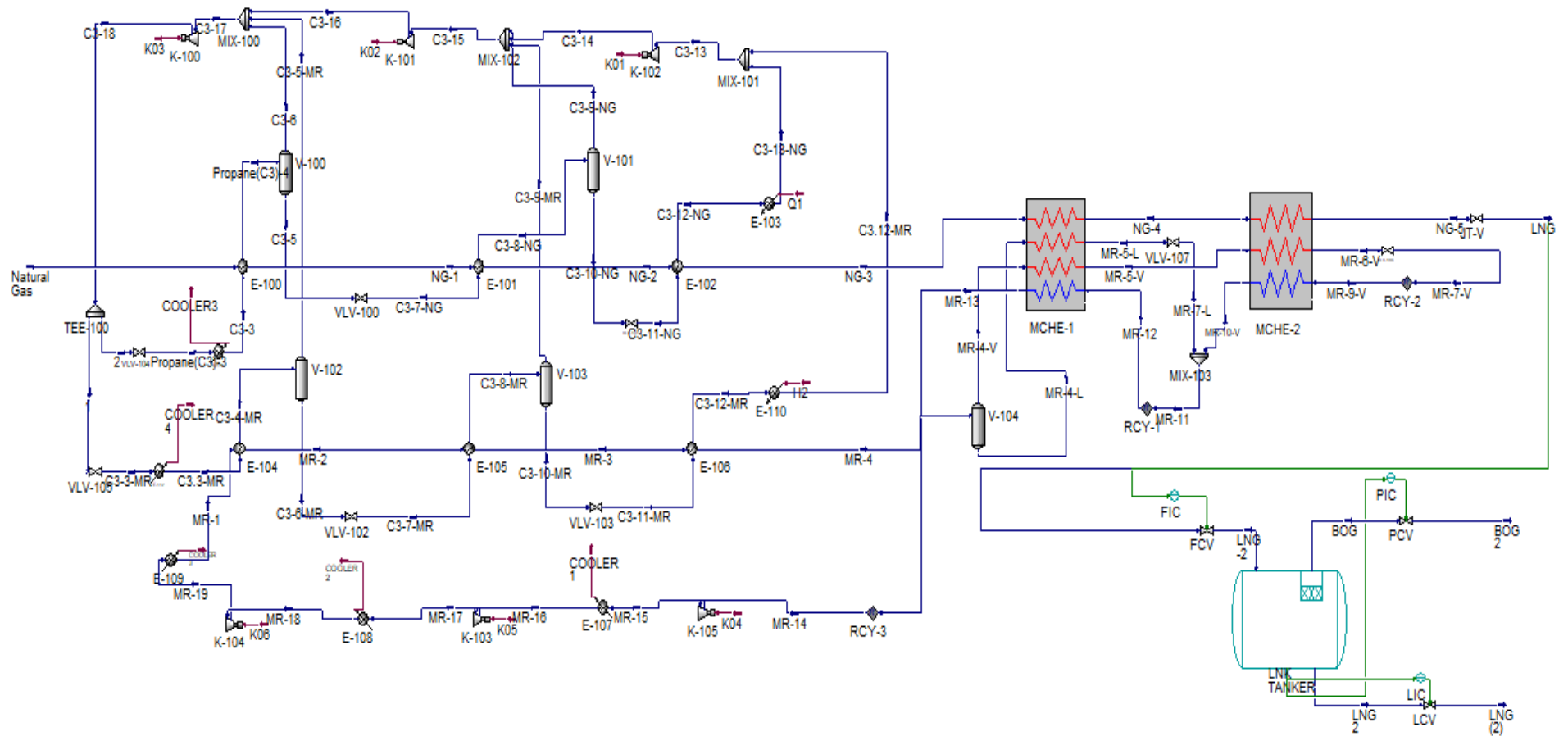


Figure 24: Liquefied Natural Gas Production (C3MR) and Storage Train.

The heat exchangers used in the pre-cooling cycle are designed as shell-and-tube heat exchangers, a pressure drop of 0.5 bar was defined for each heat exchanger.

Produced LNG is then sent to a storage tank where boil-of gas production will be estimated using the Dynamics feature of Aspen HYSYS as described in the next section. Properties of independent stream of the LNG flowsheet will be given in Appendix B.

The composition of the natural gas is the same used for DME production; presented on section 6. The composition of mixed refrigerant is shown in Table 7 based on the work done by Helgestad (2009).

Table 7: Mixed Refrigerant composition (Helgestad, 2009)

Component	Composition
Methane	45 %
Ethane	45%
Propane	2%
Nitrogen	8%

3.1.3 BOIL OFF GAS ESTIMATION

For the estimation of BOG, Dynamics feature of Aspen HYSYS was used. A steady state simulation doesn't account for a variation of a property along time, unlike Dynamic simulation.

To perform the simulation, both liquids (DME and LNG) were sent to a storage tank, simulated as a separation vessel. To better mimic the conditions of a storage vessel, which are zero flow inlet and zero flow out, three (3) Proportional Integral Derivative (PID) controllers are considered. For the inlet, a flow control valve (FCV) coupled with a PID controller (Flow Indicator Controller - FIC) were set having the inlet flow as the process variable (PV). For the liquid outlet flow, a level control valve (LCV) coupled with PID controller (Level Indicator Controller – LIC) were set defining the tank liquid level as the process variable. Finally, a pressure control valve (PCV) coupled with a PID controller, using the vessel pressure as PV is installed in the vapor outlet to count the pressure increase that will be understood as a result of BOG production. Figure 25 depicts this arrangement that was used for LNG and dimethyl ether BOG estimation.

At first stage a steady simulation is run and in sequence a dynamic simulation comes into play. For the dynamic simulation, FCV and LCV were simulated in the closed position, meaning zero flow of liquids in and out the storage tank. The BOG production is mainly due to heat transfer from the ambient to the tank surface, thus, to mimic real situation the storage tank dimensions and characteristics: thickness of insulation, conductivity of insulation and conductivity of tank surface were defined based on the work of Widodo & Muharam (2023) for better estimation of the heat transfer process as well as the BOG production.

Widodo & Muharam (2023) performed a simulation of boil-off gas recovery and fuel gas optimization with data from a real plant. The same data, regarding storage tanks geometry and heat transfer were used in this research in order to bring the estimation to a more realistic level.

The pressure increase in the vessel is an indication of the buildup of vapors boiling of the liquid. The pressure profile produced in the dynamic simulation during, 30 days at different ambient temperature were to identify the BOG production rate for both fuels.

The scheme used in the dynamic simulation is shown in Figure 25 and the heat transfer data in Table 8.

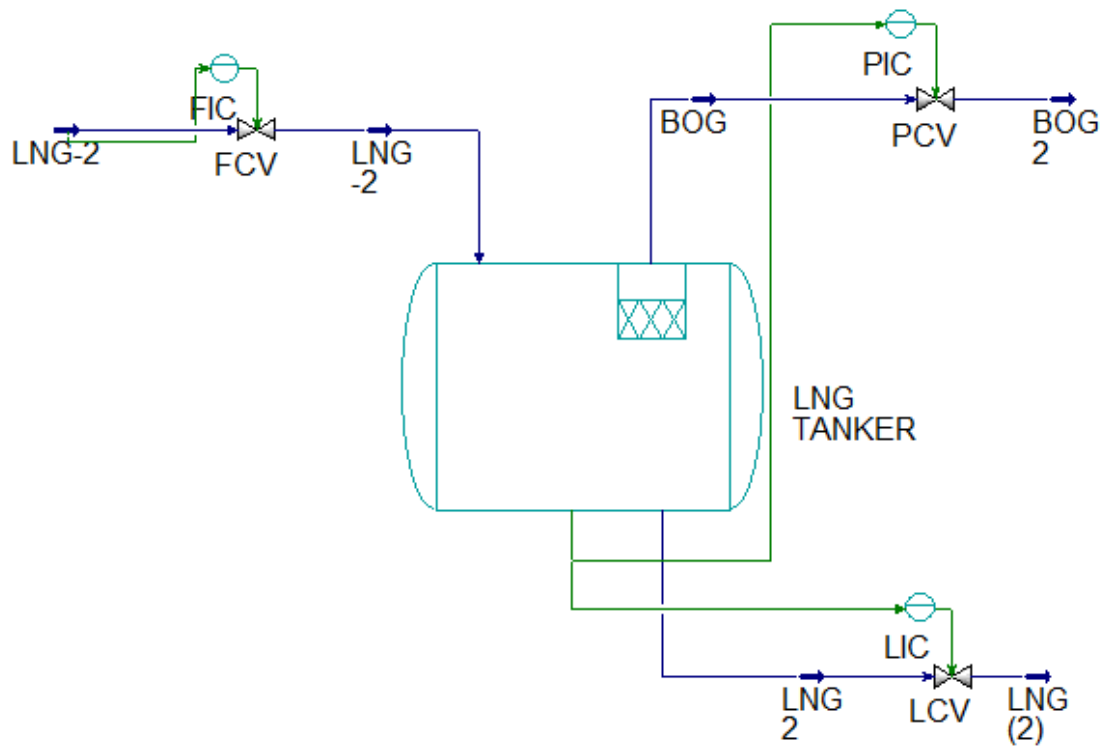


Figure 25: Boil-of gas train (dynamic simulation). The same scheme is valid for DME boil-of gas estimation.

Table 8: Storage tank properties and geometry (Helgestad, 2009)

Material		k (W/ mK)	t (cm)
Wall	Ni Steel	18.3	4
Isolation	Perlite	0.029	80
Tank Geometry			
Height (m)	42		
Internal diameter (m)	72.37		

CHAPTER IV

4. RESULTS AND DISCUSSION

In this chapter, simulation results regarding the process considered in this research are presented. For the simulation itself, the results and operating conditions for each individual streams are presented in the Appendices. The following subchapters discuss the performance of each process, the comparison of both process regarding boil of gas production, energy intensity and greenhouse gas emission.

4.1 DIMETHYL ETHER PRODUCTION PROCESS

A determinant step in DME production is the distillation column. In this unit, the DME must be separated from the liquid mixture apart from the by-products methanol and water. Figure 26 depicts how DME concentration changes along the trays of the distillation column.

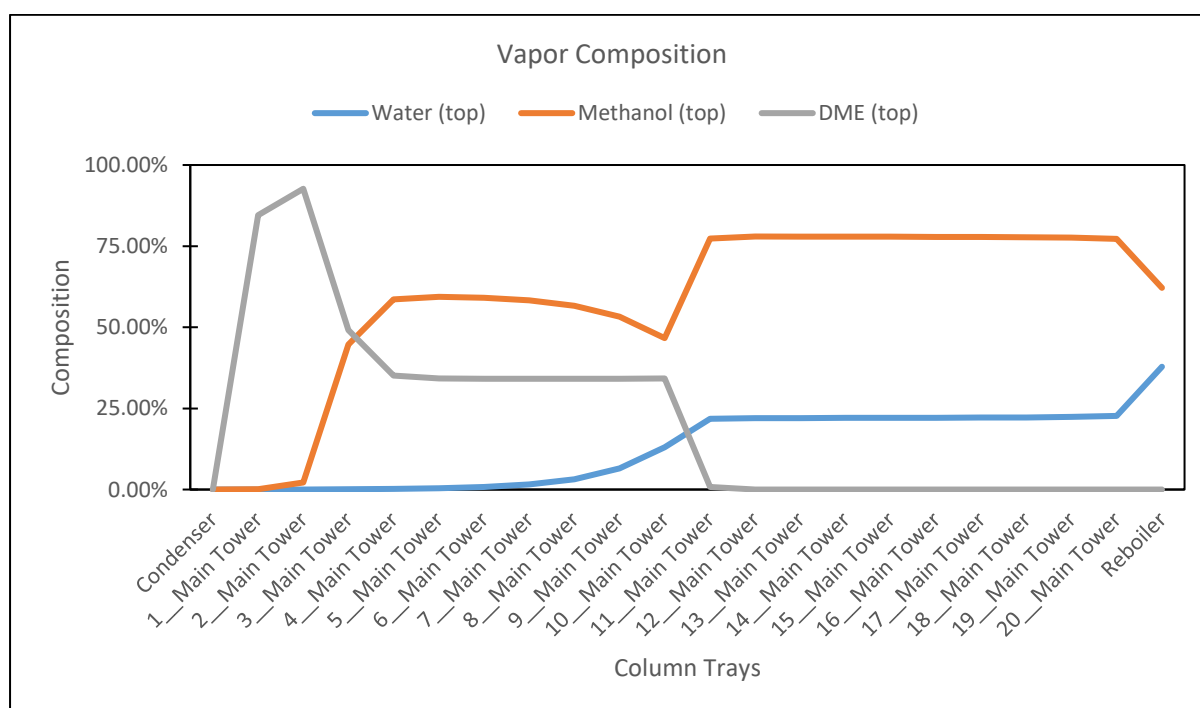


Figure 26: DME vapor stream concentration profile.

The vapor composition profiles observed across the distillation column (Figure 26) clearly illustrate the separation efficiency of the three components: DME, Methanol, and Water, based on their relative volatilities. DME, is the most volatile and thus; has a high concentration in the

top trays; its concentration declines sharply as the vapor moves through the column, indicating effective removal in the top stages. Methanol, with its intermediate volatility, is the dominant component in the middle trays, reflecting its balanced tendency to remain in the vapor phase while being separated from the DME. Water, the least volatile of the three, shows minimal presence in the top section but progressively increases in concentration as it moves downward.

This distinct separation pattern aligns with theoretical expectations for multicomponent distillation, demonstrating that the column effectively concentrates DME at the top, enriches methanol in the middle sections, and accumulates water at the bottom, thus validating both the design and operational efficiency of the distillation process.

For the liquid stream, Figure 27 depicts the composition profiles. The liquid composition profiles across the distillation column provide a complementary view to the vapor phase, highlighting the distribution of Water, Methanol, and DME in the liquid phase as they move through the column.

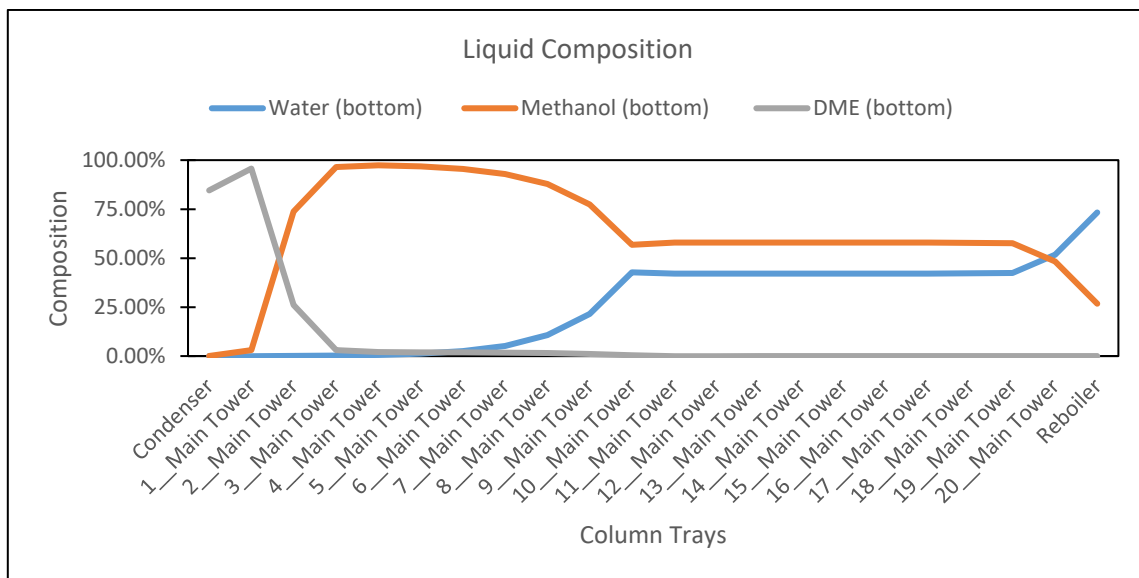


Figure 27: DME liquid composition profile.

Initially, DME is the most volatile and is therefore, highly concentrated in the liquid phase near the top trays, but it rapidly declines as it is stripped out and passes to the vapor phase. Methanol exhibits a strong presence throughout the column, especially in the middle trays, where its concentration peaks, indicating that it remains significant in the liquid phase due to its intermediate volatility. Water, with the lowest volatility, gradually increases in concentration

as it moves toward the bottom of the column, becoming the dominant component near the reboiler. This profile indicates effective separation, with DME being largely removed from the liquid phase early in the column, methanol achieving a balanced distribution, and water accumulating towards the bottom, consistent with its expected behavior in distillation. These results reinforce the operational efficiency of the column, ensuring that the least volatile component, water, is concentrated in the reboiler, while the more volatile DME is effectively separated and removed at the top.

4.2 LIQUEFIED NATURAL GAS PRODUCTION PROCESS

The hot and cold composite curves for the first Main Cryogenic Heat Exchanger (MCHE) in the LNG production process provide a detailed view of the heat exchange. It is essential for optimizing energy efficiency in this process. Figure 28 shows the composite curves for the MCHE – 1.

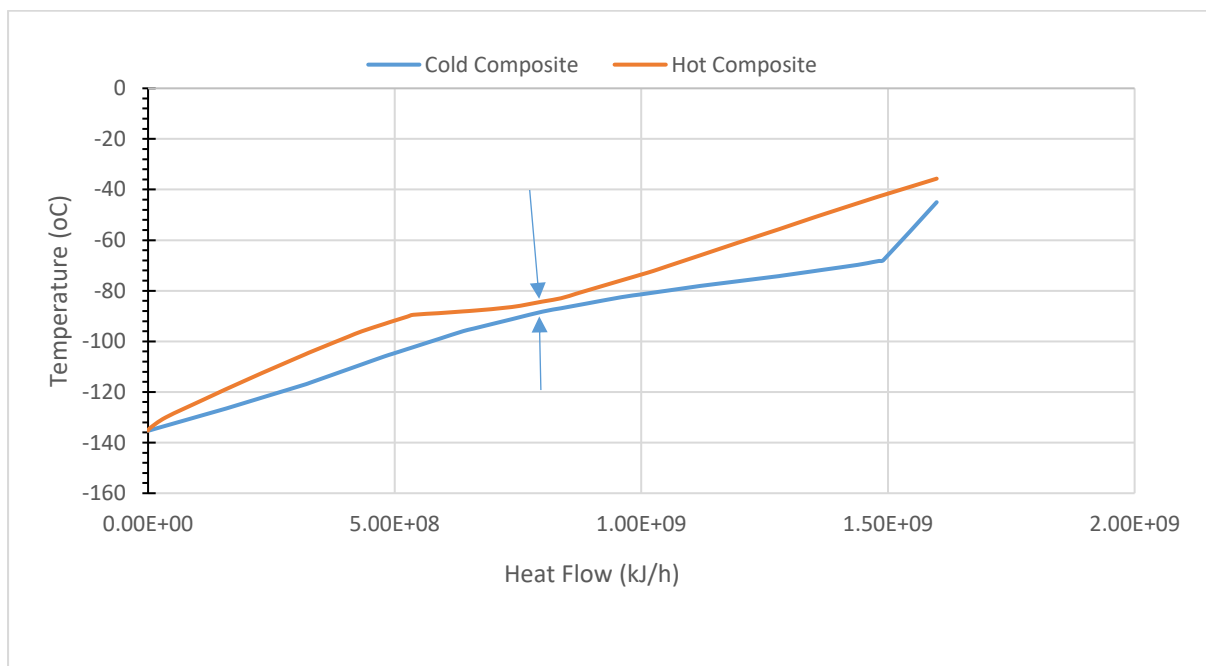


Figure 28: MCHE - 1 composite curves.

The cold composite curve (mixed refrigerants), starting at an extremely low temperature of approximately -140°C , depicts the intensive cooling required to liquefy natural gas (hot composite). As the heat is absorbed by the mixed refrigerant (MR), its temperature increases gradually, a crucial step in achieving the deep cryogenic conditions for the Liquefaction of

natural gas. As the heat is transferred to the MR, the temperature of the natural gas decreases progressively, aligning with the requirements of the LNG process.

The proximity of the two curves over a substantial range of heat flow indicates a high degree of heat integration within the MCHE. The pinch point, where the temperature difference between the hot and cold streams is at its minimum, is particularly important. This critical point dictates the overall energy efficiency of the exchanger; managing it carefully can significantly reduce energy consumption and operational costs. In the MCHE – 1 the natural is cooled to -135 °C.

Figure 29 shows the composite curves of the MCHE – 2. Here, the natural gas is cooled from -135 °C to -155 °C, as it is depicted by the hot composite curve. Once more, the closeness of the two curves indicates how efficient is the heat exchanging process in the MCHE – 2.

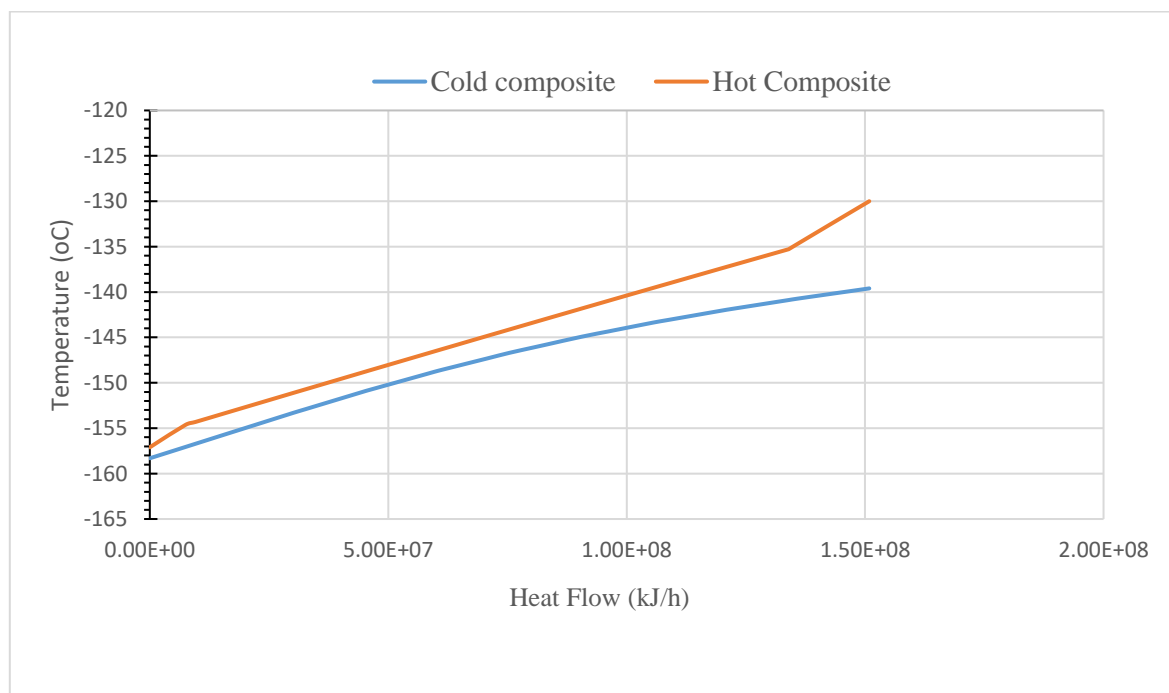


Figure 29: MCHE - 2 composite curves.

The effective design of these MCHE, as demonstrated by the composite curves, ensures that the heat exchange process is optimized to absorb as much energy as possible, which is crucial in lowering the operational costs associated with LNG production. The well-defined overlap between the hot and cold composites indicates that the exchanger is operating close to its thermodynamic limits, maximizing energy recovery and minimizing waste. These findings, the

composites curves profile and their effects are also backed up by the study done by (Helgestad, 2009). This efficient heat integration is essential not only for reducing the environmental impact of the LNG production process but also for maintaining competitiveness in an industry where energy costs are a major factor, since closer curves means less heat transfer area.

4.3 ENERGY INTENSITIES AND GREENHOUSE GAS EMISSION COMPARISON

4.3.1 ENERGY ANALYSIS OF DIMETHYL ETHER PRODUCTION

The production of DME presents itself as a process with very high energy intensity as well as CO₂ emissions. The selected technology for this research encompasses DME production from natural gas including syngas production. Figure 30 shows that the total energy usage for DME production is in the order of 100 GJ/tonne of DME, which is a huge amount of energy.

The energy intensity value mostly comes from the syngas production process, in the pre-reforming and reforming section. The reactions that convert natural gas to CO and H₂ are endothermic in nature and occur at high temperatures (650 – 850 °C), meaning that a substantial amount of thermal energy must be supplied to break the methane molecule and reform it to syngas. To achieve the ideal CO/H₂ ratio an autothermal reformer was used. Besides this unit, the DME distillation column also has a reboiler that requires heating. To minimize this energy demand, heat integration approaches should have been done, however, it was out the scope of the research, since it would make the simulation flowsheet more complex, taking more simulation time for the results.

According to the results in Figure 30, the total energy intensity is 100 GJ/tonne of DME, however, if one decides to apply energy integration approaches to the same flowsheet, by using heat exchangers to recovery residual energy from the process streams, this value could be reduced to 37.90 GJ/tonne of DME. This simply means, that in an optimized and heat integrated flowsheet, the energy intensity of DME production could be 37.90 GJ/tonne.

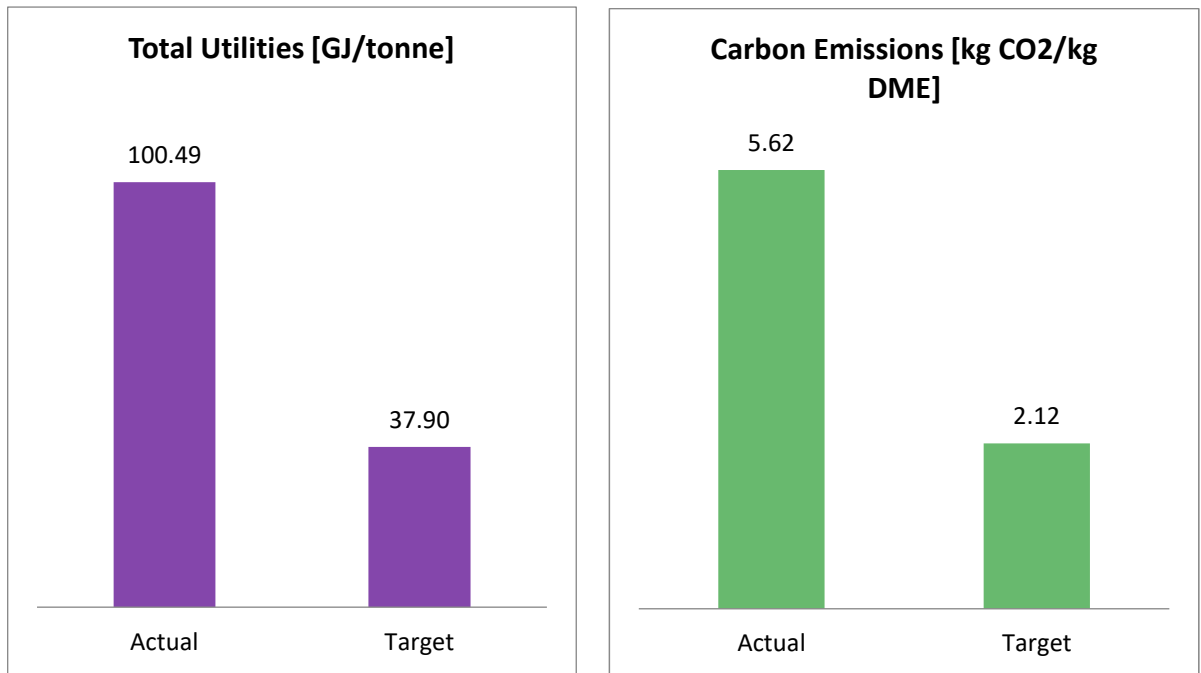


Figure 30: DME production process energy and GHG analysis.

The same analysis can be done looking at the Green House Gas emissions (represented by CO₂ equivalent emissions). For this part, the simulator assumes that all heating used in the simulation is produced from fossil fuels (when running heaters as unit operation), and then it sums all the CO₂ emissions, from process emissions to emission in electricity production.

The actual intensity of the process is 5.62 kgCO₂/kg of DME, counting process emissions (mainly from reforming reaction, combustion gases from fuel gas combustion in the reformer and CO₂ from electricity generation used in heaters). Similarly, if heat integration was used, some heaters would have been avoided and reduced the emissions to 2.12 kgCO₂/kg of DME, which is close to 1,8 kgCO₂/kg of DME reported by Poto et al. (2023).

Thus, for any optimized process of DME production, one can expect 37.90 GJ/tonne for energy intensity and 2.12 kgCO₂/kg of DME for CO₂ intensity, which are reasonable values. This also shows how important is the heat recovery in the overall energy efficiency framework for a production process, and how it can impact on the environmental scenario.

4.3.2. ENERGY ANALYSIS FOR THE LIQUEFIED NATURAL GAS PRODUCTION

Differently from the DME production flowsheet, the LNG flowsheet was carried out using a heat integration approach, due to the intrinsic nature of cryogenic plants. Typically, LNG production plants are characterized by a high degree of energy reuse to reduce as much as possible the energy demand, and this can be seen in the flowsheet depicted on Figure 24.

In figure 31 one can see that the LNG train has a GHG emissions of 1.22 kgCO₂/kg of LNG. This emission comes from the heaters used to remove liquids droplets of the MR before entering the compressors, since the vaporization in the precooling heat exchangers were not 100 % complete. Aspen HYSYS assumes that heat used in the heaters and compressors comes from a fossil fuel source and calculates the associated CO₂ emissions. One can also see that the actual and target values for the CO₂ emission are almost equal, meaning that the process is highly optimized.

Howarth (2024), states that a total carbon footprint of a liquefaction plant can be estimated by adding the following specifics emissions: 612 gCO₂/kg of LNG to drive the compressors that transport natural gas from; 270 to 410 gCO₂/kg of LNG during liquefaction process (MR compressors) and a maximum of 50 gCO₂/kg of LNG for flaring. Thus, according to Howarth (2024) the CO₂ emissions in LNG production ranges from 0.932 to 1.1 kgCO₂/kg of LNG, excluding CO₂ that comes with natural gas itself. Hence, the results obtained are in agreement with previous estimations.

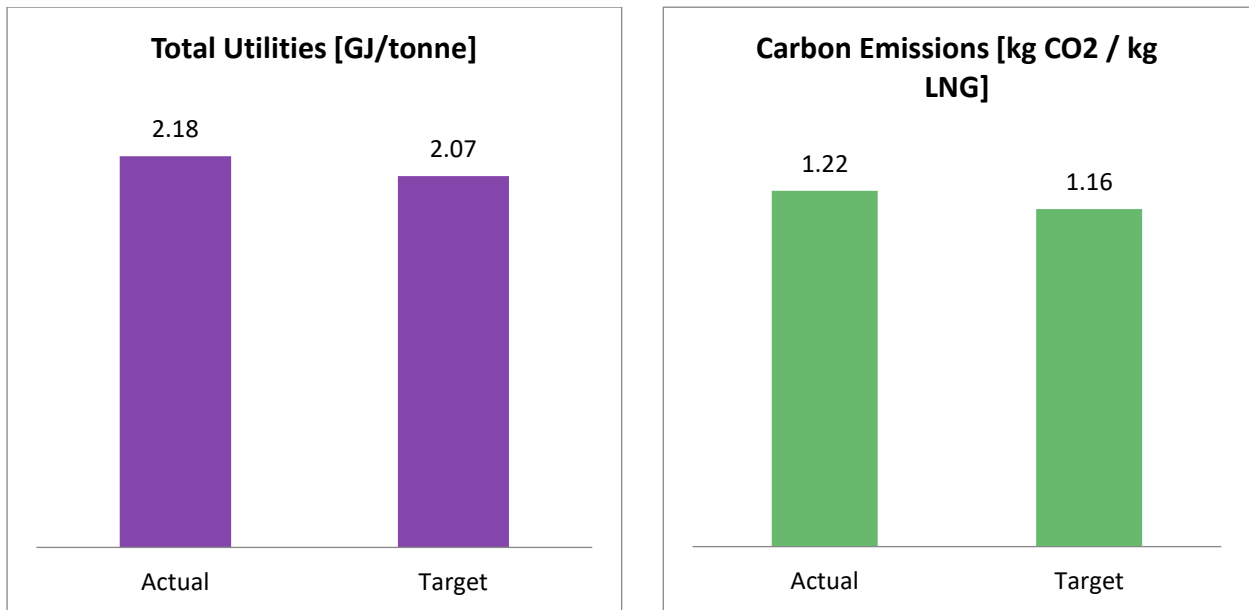


Figure 31: LNG production process energy and GHG analysis.

For the reason stated above, one can also see that the actual energy intensity and target energy intensity are values almost equal. This happens, because an intensive heat integration approach was taken to recover almost of the heat, by crossing the heat and cold utilities through heat exchangers and economizers. These results show how efficient is the LNG production technology chosen for this research. According to the study done by Zonfrilli et al. (2023); the energy intensity of a liquefaction plants ranges from 1.1 GJ/tonne to 3 GJ/tonne of LNG depending on the technology selected. In this research, the target energy intensity is 2.07 GJ/tonne of LNG, which shows agreement range in values provided by Zonfrilli et al. (2023).

4.4 BOIL OFF GAS PRODUCTION COMPARISON

In order to compare the boil off gas rate of production, the LNG and DME were stored under the same conditions, i.e storage size, tank material, type of isolation and external ambient temperature. The following results (Figure 32 and Figure 33) depicts the BOG production for both LNG and DME, considering an ambient temperature outside the storage tanks of 30 °C. The BOG production is depicted in terms of pressure build up for 15 days of storage.

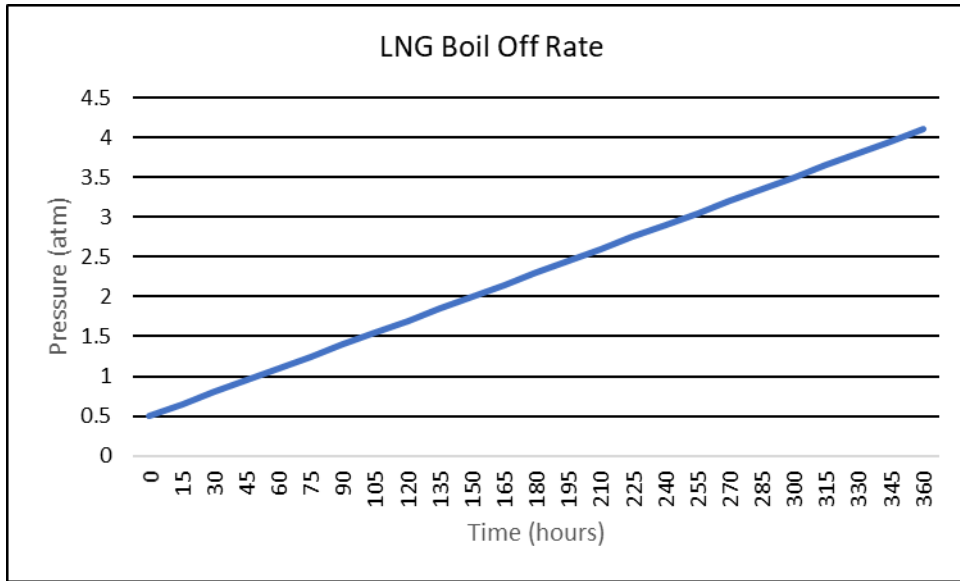


Figure 32: LNG boil off gas production.

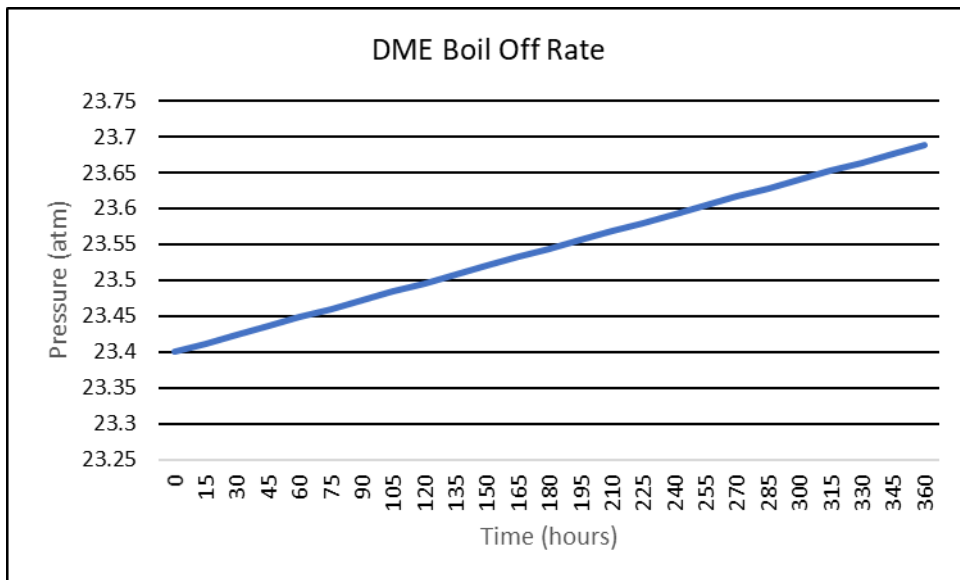


Figure 33: DME boil off gas production.

Figure 32 shows that in the LNG storage tank, the pressure increases from 0.5 atm to 4.1 atm, which is a substantial increase in pressure that might compromise the physical integrity of the storage vessel. This sustains the importance of having pressure relief valves in LNG storage tanks, since the pressure can increase by a factor of 9, for this case. Similarly, Kalikatzarakis et al. (2022) reported similar results for pressure build-up inside a tank.

Figure 33 shows that DME produces as much as almost nothing in terms of BOG. The pressure keeps almost the same during the 15 days, moving from 23.4 atm to 23.7 atm, a marginal growth. Similarly, Al-Breiki & Bicer (2020); observed that DME had a BOG. These results can be attributed to several thermophysical properties and storage conditions of both liquids. One of the primary reasons for DME lower BOG rate is its relatively higher boiling point of approximately -25°C at atmospheric pressure, which reduces the thermal gradient between the storage environment and the liquid. The small temperature differential minimizes the rate of heat ingress into the storage tank, thus reducing the rate of vaporization of DME compared to LNG, the latter having a boiling point of around -162°C .

In addition, DME exhibits a higher latent heat of vaporization (19.6 kJ/mol) relative to LNG (14.7 kJ/mol), meaning that a greater amount of energy is required to convert a unit mass of DME from liquid to vapor. This property contributes to the lower BOG rate, as the same amount of heat ingress causes lesser evaporation in DME than in LNG. The uniformity in the composition of DME, being a single-component fluid, also plays a role in maintaining a consistent boil-off rate.

The findings from this research underscore that the lower BOG rate of DME is inherently tied to its higher boiling point and higher latent heat of vaporization, all of which collectively lead to more efficient and stable storage conditions with reduced evaporative losses.

The results shown in Figure 34 and Figure 35 highlight the different simulation results from LNG production and the experimental results.

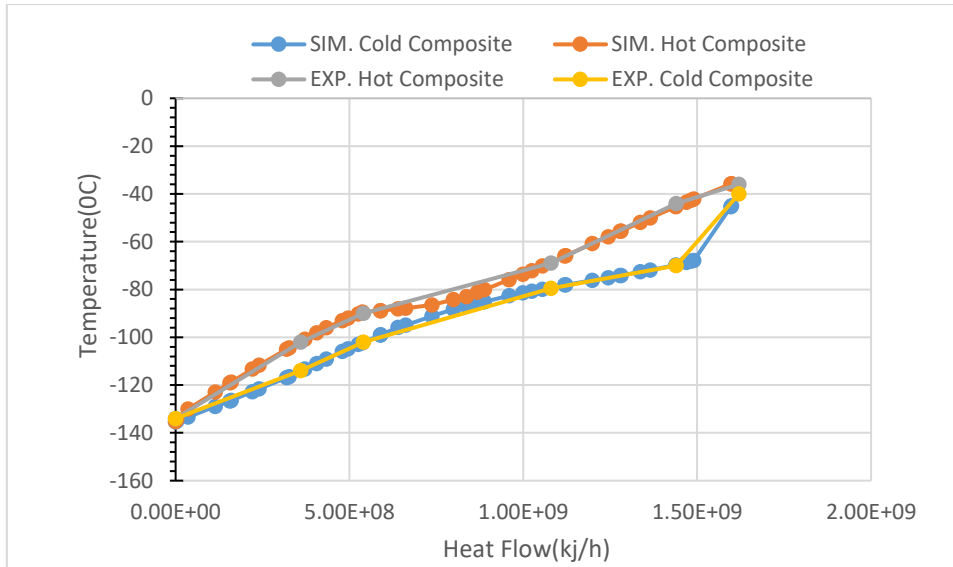


Figure 34: Simulation and experiments result in MCHE -1

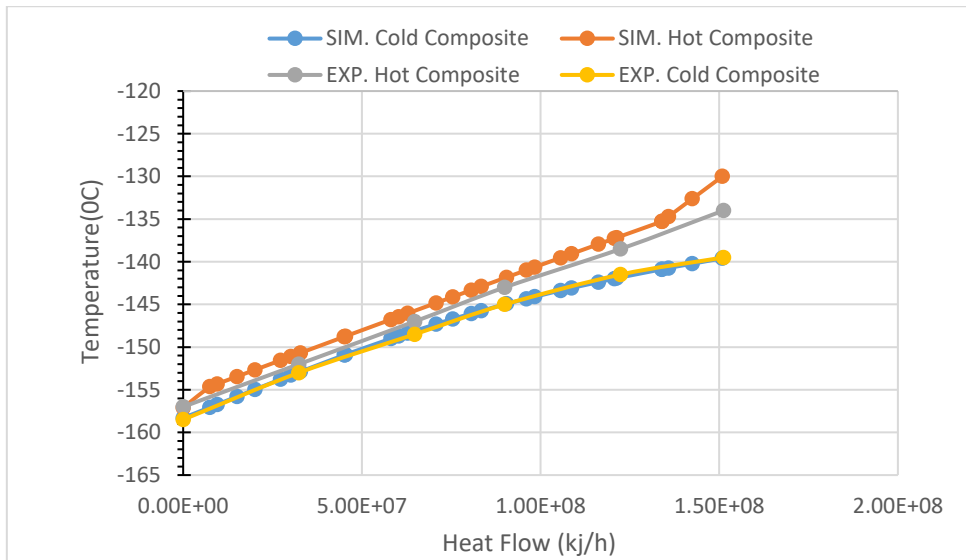


Figure 35: Simulation and experiment results in MCHE -2

The temperature profile showing the cold and hot composite of the results obtained from simulation and the experiments conducted by (Helgestad, 2009) researchers for the two parts of the MCHE. Our simulation results show agreement with experimental results although minor deviations are evident. After comparing simulation results with experimental data carried out by other researchers, the observed agreement between the simulation and experimental results validates our approach and confirms that the simulation correctly represents the physical processes observed in the experiments.

CHAPTER V

5. CONCLUSION AND RECOMMENDATIONS

5.1 CONCLUSION

Based on the simulation results, the research successfully achieved its objectives by developing and simulating production processes for both Dimethyl Ether (DME) and Liquefied Natural Gas (LNG).

The findings reveal that:

- LNG has a much higher boil-off gas (BOG) rate than DME, with LNG's pressure increasing significantly from 0.5 atm to 4.1 atm over 15 days.
- DME pressure rise only slightly from 23.4 atm to 23.7 atm. This shows that DME is more stable and better suited for long-term storage with minimal evaporative loss.
- DME production has higher energy intensity of 37.9 GJ/tonne and CO₂ emissions of 2.12 kg CO₂/kg compared to LNG's lower energy intensity of 2.07 GJ/tonne and emissions of 1.16 kg CO₂/kg.

These results suggest that while DME offers benefits in terms of lower BOG rates, it has a higher energy penalty and greater environmental impact, reminding the need for further optimization in its production process to improve its overall energy efficiency and sustainability. Thus, the choice between DME and LNG production pathways depends on the specific priorities of the application, whether it be minimizing evaporative losses or reducing energy consumption and emissions.

5.2 RECOMMENDATIONS

Based on the findings and limitations of this study, the following recommendations are made for future research:

- Future studies should extend beyond the technical feasibility explored in this dissertation to include a comprehensive economic analysis of DME and LNG production. This should encompass capital and operational expenditures, cost comparisons between the two production pathways.
- While this research focused on CO₂ emissions, further investigation is needed to explore the broader environmental impacts of DME and LNG production. Future research could evaluate the impact of integrating carbon capture and storage (CCS) technologies to DME production.
- Given the higher energy intensity and CO₂ emissions associated with DME production, future studies should focus on energy integration approaches to increase the energy efficiency of the DME process.

REFERENCES

- Al-Breiki, M., & Bicer, Y. (2020). Investigating the Effects of Boil-off Gas on Liquefied Energy Carriers during Land Storage and Ocean Transportation. *IOP Conference Series: Earth and Environmental Science*, 581(1). <https://doi.org/10.1088/1755-1315/581/1/012017>
- Azarhoosh, M. J., Ale Ebrahim, H., & Pourtarah, S. H. (2015). Simulating and optimizing hydrogen production by low-pressure autothermal reforming of natural gas using non-dominated sorting genetic algorithm-II. *Chemical and Biochemical Engineering Quarterly*, 29(4), 519–531. <https://doi.org/10.15255/CABEQ.2014.2158>
- Azizi, Z., Rezaeimanesh, M., Tohidian, T., & Rahimpour, M. R. (2014). Dimethyl ether: A review of technologies and production challenges. *Chemical Engineering and Processing: Process Intensification*, 82, 150–172. <https://doi.org/10.1016/j.cep.2014.06.007>
- Banivaheb, S., Pitter, S., Delgado, K. H., Rubin, M., Sauer, J., & Dittmeyer, R. (2022). Recent Progress in Direct DME Synthesis and Potential of Bifunctional Catalysts. *Chemie-Ingenieur-Technik*, 94(3), 240–255. <https://doi.org/10.1002/cite.202100167>
- Bassioni, G., & Klein, H. (2023). Liquefaction of natural gas and simulated process optimization – A review. *Ain Shams Engineering Journal*, 15(December 2022). <https://doi.org/10.1016/j.asej.2023.102431>
- Bouabidi, Z., Almomani, F., Al-Musleh, E. I., Katebah, M. A., Hussein, M. M., Shazed, A. R., Karimi, I. A., & Alfadala, H. (2021). Study on boil-off gas (Bog) minimization and recovery strategies from actual baseload lng export terminal: Towards sustainable lng chains. *Energies*, 14(12). <https://doi.org/10.3390/en14123478>
- Brunetti, A., Scura, F., Barbieri, G., & Drioli, E. (2010). Membrane technologies for CO₂ separation. *Journal of Membrane Science*, 359(1–2), 115–125. <https://doi.org/10.1016/j.memsci.2009.11.040>
- Dobrota, Đ., Lalić, B., & Komar, I. (2013). Problem of Boil - off in LNG Supply Chain.

Transactions on Maritime Science, 2(2), 91–100.
<https://doi.org/10.7225/toms.v02.n02.001>

Ezeh, P., K. Dagde, K., & G. Akpa, J. (2019). Computer Aided Design for the Recovery of Boil-Off Gas from LNG Plant. *Advances in Chemical Engineering and Science*, 09(02), 159–175. <https://doi.org/10.4236/aces.2019.92012>

Fortin, C., Gianfolcaro, N., Gonzalez, R., Lohest, J., Lonneux, A., Mordant, P., Kesnelle, A., Siliki, N., Peiffer, T., Renson, R., & Schmitz, C. (2020). Dimethyl ether, A review of production processes and a modeling of the indirect route. *Liege Univeristy*, 12(1), 3–14. https://www.chemeng.uliege.be/upload/docs/application/pdf/2020-05/projetdme_finalreport.pdf

Franceus et. al. (1999). Increase the Feedstock Flexibility of an Ammonia Plant Production Facility by Installing a Pre-reformer Unit. *AIChE Ammonia Safety Symposium*.

Gogate, M. R. (2018). The direct, one-step process for synthesis of dimethyl ether from syngas. III. DME as a chemical feedstock. *Petroleum Science and Technology*, 36(8), 562–568. <https://doi.org/10.1080/10916466.2018.1428630>

Hasan, M. M. F., Zheng, A. M., & Karimi, I. A. (2009). Minimizing boil-off losses in liquefied natural gas transportation. *Industrial and Engineering Chemistry Research*, 48(21), 9571–9580. <https://doi.org/10.1021/ie801975q>

Helgestad, D. (2009). Modelling and optimization of the C3MR process for liquefaction of natural gas. *Process System Engineering*. https://folk.ntnu.no/skoge/diplom/prosjekt09/helgestad/Helgestad_project.pdf

Howarth, R. W. (2024). *The greenhouse gas footprint of liquefied natural gas (LNG) exported from the United States. September*. <https://doi.org/10.1002/ese3.1934>

Jafari, M., Vatani, A., Deljoo, M.S., Khalili- Garakani, A. (2021). Techno-Economic Analysis of Flare Gas to Gasoline (FGTG) Process through Dimethyl Ether Production. *Journal of Gas Technology*, 6(2), 28–44.

Jensen, J. B., & Skogestad, S. (2006). Optimal Operation of a Simple Lng Process. In *IFAC*

Proceedings Volumes (Vol. 39, Issue 2). IFAC. <https://doi.org/10.3182/20060402-4-br-2902.00241>

Jung, M., & Corporation, K. G. (2000). *Lng Terminal Design Feedback*.

Kalikatzarakis, M., Theotokatos, G., Coraddu, A., Sayan, P., & Wong, S. Y. (2022). Model based analysis of the boil-off gas management and control for LNG fuelled vessels. *Energy*, 251, 123872. <https://doi.org/10.1016/j.energy.2022.123872>

Karagoz, S. (2014). *Process Design, Simulation and Integration of Dimethyl Ether (Dme) Production From Shale Gas By Direct and Indirect Methods*. August, 1–75.

Kelechi, C., Akpa, J. G., & Ehirim, E. O. (2022). *Simulation and Optimization of Natural Gas Sweetening Plant*. August. <https://doi.org/10.13140/2.1.4347.0720>

Kim, K., Park, K., Roh, G., & Chun, K. (2019). Case study on boil-off gas (BOG) minimization for lng bunkering vessel using energy storage system (ESS). *Journal of Marine Science and Engineering*, 7(5). <https://doi.org/10.3390/jmse7050130>

Kurle, Y. M., Wang, S., & Xu, Q. (2015). Simulation study on boil-off gas minimization and recovery strategies at LNG exporting terminals. *Applied Energy*, 156, 628–641. <https://doi.org/10.1016/j.apenergy.2015.07.055>

Lee, I., Park, J., & Moon, I. (2018). Key Issues and Challenges on the Liquefied Natural Gas Value Chain: A Review from the Process Systems Engineering Point of View. *Industrial and Engineering Chemistry Research*, 57(17), 5805–5818. <https://doi.org/10.1021/acs.iecr.7b03899>

Lim, W., Choi, K., & Moon, I. (2012). *Current Status and Perspectives of Liquefied Natural Gas (LNG) Plant Design*. 6.

Makos, P., Słupek, E., Sobczak, J., Zabrocki, D., Hupka, J., & Rogala, A. (2019). Dimethyl ether (DME) as potential environmental friendly fuel. *E3S Web of Conferences*, 116. <https://doi.org/10.1051/e3sconf/201911600048>

Manaças, V. H. C. (2013). Advanced steady-state modelling and optimisation of Natural Gas

- Reforming reactors Chemical Engineering Examination Committee. *University of Lisbon, Portugal (Master's Thesis), December, 1–10.*
- Mokhatab, S., Poe, W. A., & Mak, J. Y. (2015). Natural Gas Liquids Recovery. In *Handbook of Natural Gas Transmission and Processing*. <https://doi.org/10.1016/b978-0-12-801499-8.00008-0>
- Nie, Z., Liu, H., Liu, D., Ying, W., & Fang, D. (2005). Intrinsic kinetics of dimethyl ether synthesis from syngas. *Journal of Natural Gas Chemistry, 14*(1), 22–28.
- Noureldin, M. M. B., Elbashir, N. O., & El-Halwagi, M. M. (2014). Optimization and selection of reforming approaches for syngas generation from natural/shale gas. *Industrial and Engineering Chemistry Research, 53*(5), 1841–1855. <https://doi.org/10.1021/ie402382w>
- Numaguchi, T., & Kikuchi, K. (1988). Intrinsic kinetics and design simulation in a complex reaction network; steam-methane reforming. *Chem. Eng. Sci.* [https://doi.org/http://dx.doi.org/10.1016/0009-2509\(88\)87118-5](https://doi.org/http://dx.doi.org/10.1016/0009-2509(88)87118-5)
- Ogawa, T., Inoue, N., Shikada, T., Inokoshi, O., & Ohno, Y. (2004). Direct Dimethyl Ether (DME) synthesis from natural gas. *Studies in Surface Science and Catalysis, 147*, 379–384. [https://doi.org/10.1016/s0167-2991\(04\)80081-8](https://doi.org/10.1016/s0167-2991(04)80081-8)
- Otaraku, I. J., & Onyekaonwu, C. (2018). Process Design of Associated Natural Gas to Dimethyl Ether Production Via Direct Synthesis. *International Journal of Chemical and Process Engineering Research, 5*(1), 1–7. <https://doi.org/10.18488/journal.65.2018.51.1.7>
- Park, C., Lee, C. J., Lim, Y., Lee, S., & Han, C. (2010). Optimization of recirculation operating in liquefied natural gas receiving terminal. *Journal of the Taiwan Institute of Chemical Engineers, 41*(4), 482–491. <https://doi.org/10.1016/j.jtice.2010.04.014>
- Poto, S., Vink, T., Oliver, P., Gallucci, F., & Neira, M. F. (2023). Techno-economic assessment of the one-step CO₂ conversion to dimethyl ether in a membrane-assisted process. *Journal of CO₂ Utilization, 69*(December 2022), 102419. <https://doi.org/10.1016/j.jcou.2023.102419>

- Rice, S. F., & Mann, D. P. (2007). Autothermal Reforming of Natural Gas to Synthesis Gas. *Sandia Report, 125*(April), 50.
- Sedlacek, R. (2008). BOIL-OFF IN LARGE- AND SMALL-SCALE LNG CHAINS. *Faculty of Engineering Science and Technology Department of Petroleum Engineering and Applied Geophysics, May*.
- Seungjune, C., Jehun, P., Chonghun, H., & En, S. Y. (2008). Optimal design of synthesis gas production process with recycled carbon dioxide utilization. *Industrial and Engineering Chemistry Research, 47*(2), 323–331. <https://doi.org/10.1021/ie070961n>
- Speight, J. G. (2015). *HANDBOOK OF OFFSHORE OIL AND GAS OPERATIONS* (1st ed.).
- Widodo, A., & Muharam, Y. (2023). Simulation of boil-off gas recovery and fuel gas optimization for increasing liquefied natural gas production. *Energy Reports, 10*(April), 4503–4515. <https://doi.org/10.1016/j.egy.2023.11.003>
- Wu, M., Zhu, Z., Sun, D., He, J., Tang, K., Hu, B., & Tian, S. (2019). Optimization model and application for the recondensation process of boil-off gas in a liquefied natural gas receiving terminal. *Applied Thermal Engineering, 147*, 610–622. <https://doi.org/10.1016/j.applthermaleng.2018.10.117>
- Xu, J., & Froment, G. F. (1989). Methane steam reforming, methanation and water-gas shift: I. Intrinsic kinetics. *AIChE Journal, 35*(1), 88–96. <https://doi.org/10.1002/aic.690350109>
- Yuan, Z., Cui, M., Xie, Y., & Li, C. (2014). Design and analysis of a small-scale natural gas liquefaction process adopting single nitrogen expansion with carbon dioxide pre-cooling. *Applied Thermal Engineering, 64*(1–2), 139–146. <https://doi.org/10.1016/j.applthermaleng.2013.12.011>
- Zahedi nezhad, M., Rowshanzamir, S., & Eikani, M. H. (2009). Autothermal reforming of methane to synthesis gas: Modeling and simulation. *International Journal of Hydrogen Energy, 34*(3), 1292–1300. <https://doi.org/10.1016/j.ijhydene.2008.11.091>
- Zhang, J., Meerman, H., Benders, R., & Faaij, A. (2020). Comprehensive review of current natural gas liquefaction processes on technical and economic performance. *Applied*

Thermal Engineering, 166(November 2019), 114736.
<https://doi.org/10.1016/j.applthermaleng.2019.114736>

Zno, C., Al, O., Aguayo, T., Eren, J., Mier, D., Arandes, M., Olazar, M., & Bilbao, J. (2007). *Kinetic Modeling of Dimethyl Ether Synthesis in a Single Step on a*. 5522–5530.

Zonfrilli, M., Facchino, M., Serinelli, R., Chesti, M., De Falco, M., & Capocelli, M. (2023). Thermodynamic analysis of cold energy recovery from LNG regasification. *Journal of Cleaner Production*, 420, 138443. <https://doi.org/10.1016/J.JCLEPRO.2023.138443>

APPENDICES

APPENDIX A – DME PRODUCTION DATA

Table A 1: Operating Conditions of DME production process.

Name	Natural Gas	NG-2	NG-5	Steam	NG-3	NG-4	NG-6	Fuel
Vapour Fraction	1.00	1.00	1.00	1.00	1.00	1.00	1.00	1.00
Temperature [C]	26.46	151.20	414.38	405.17	301.21	500.00	620.00	30.00
Pressure [atm]	7.90	29.61	29.61	30.00	29.61	29.61	29.61	7.90
Molar Flow [kgmole/h]	1,000.00	1,000.00	3,110.77	2,000.00	3,000.00	3,000.00	3,110.77	200.00
Mass Flow [kg/h]	17,416.34	17,416.34	53,446.59	36,030.20	53,446.54	53,446.54	53,446.59	3,483.27
Name	Air	Flue Gas	NG-7	Reformate	Reformate 1	To Absorber	Produced Water	Syngas
Vapour Fraction	1.00	1.00	1.00	1.00	1.00	1.00	0.00	1.00
Temperature [C]	25.00	1,951.42	629.39	491.28	200.00	40.00	40.00	41.11
Pressure [atm]	1.00	1.00	29.61	28.41	28.41	28.41	28.41	28.41
Molar Flow [kgmole/h]	1,900.00	2,138.54	3,110.77	3,298.42	3,298.42	1,453.44	1,844.98	371.97
Mass Flow [kg/h]	54,815.51	58,298.78	53,446.59	53,446.67	53,446.67	20,208.61	33,238.07	4,587.23
Name	PSA Off-Gas	To PSA	To Reboiler	Water	Water 2	Water 1	Water 3	Steam 1
Vapour Fraction	1.00	1.00	1.00	0.00	0.00	0.00	0.00	1.00
Temperature [C]	41.11	40.01	40.01	25.00	114.77	25.49	232.83	302.00
Pressure [atm]	28.41	28.41	28.41	1.00	80.00	80.00	80.00	80.00
Molar Flow [kgmole/h]	1,077.26	1,449.22	4.21	4,000.00	4,000.00	4,000.00	4,000.00	4,000.00
Mass Flow [kg/h]	15,527.80	20,115.04	93.57	72,060.40	72,060.40	72,060.40	72,060.40	72,060.40

Table A 2: Operating Conditions of DME production process (cont.)

Name	Flue Gas 1	Steam 2	Flue Gas 2	Steam 3	Steam to SMR	Steam 4	Steam 5	NG -1
Vapour Fraction	1.00	1.00	0.81	1.00	1.00	1.00	1.00	1.00
Temperature [C]	344.43	535.00	-7.48	405.17	405.17	405.17	120.65	26.46
Pressure [atm]	1.00	80.00	1.00	30.00	30.00	30.00	2.00	7.90
Molar Flow [kgmole/h]	2,138.54	4,000.00	2,138.54	4,000.00	2,000.00	2,000.00	2,000.00	1,000.00
Mass Flow [kg/h]	58,298.78	72,060.40	58,298.78	72,060.40	36,030.20	36,030.20	36,030.20	17,416.34
Name	To DME Reactor	DME Products	L	To distillation	To rec	To tower	DME	Methanol-H2O
Vapour Fraction	1.00	1.00	0.00	0.86	1.00	0.00	0.01	0.00
Temperature [C]	180.00	180.00	180.00	45.00	41.45	45.00	-181.14	100.88
Pressure [atm]	28.41	28.41	28.41	28.41	22.49	28.41	1.50	2.00
Molar Flow [kgmole/h]	371.97	162.64	0.00	162.64	140.28	22.36	9.21	13.15
Mass Flow [kg/h]	4,587.23	4,587.13	0.00	4,587.13	3,883.00	704.13	417.95	286.17
Name	DME PRODUCT (2)	DME TO FLASH	VAPO R	DME TO STORAGE	DME TO STORAGE (1)	DME BOG	DME (L)	DME BOG(1)
Vapour Fraction	0.01	0.00	1.00	0.00	0.00	1.00	0.00	1.00
Temperature [C]	-178.80	25.00	25.00	25.00	24.97	24.97	24.97	24.80
Pressure [atm]	25.00	24.51	24.51	24.51	24.01	24.01	24.01	23.72
Molar Flow [kgmole/h]	9.21	9.21	0.00	9.21	9.21	0.01	9.21	0.01
Mass Flow [kg/h]	417.95	417.95	0.00	417.95	417.95	0.18	417.77	0.18

Table A 3: Composition of main streams in DME production.

Name	DME PRODUCT (2)	DME TO FLASH	VAPO R	DME TO STORAG E	DME TO STORAGE (1)	DME BOG	DME (L)	DME BOG(1)
Comp Mole Frac (Methane)	0.06%	0.06%	0.55%	0.06%	0.06%	0.56%	0.06%	0.56%
Comp Mole Frac (H2O)	0.00%	0.00%	0.00%	0.00%	0.00%	0.00%	0.00%	0.00%
Comp Mole Frac (CO)	0.02%	0.02%	0.48%	0.02%	0.02%	0.48%	0.02%	0.48%
Comp Mole Frac (CO2)	14.42%	14.42%	28.28%	14.42%	14.42%	28.74 %	14.41%	28.74%
Comp Mole Frac (Hydrogen)	0.88%	0.88%	45.26%	0.88%	0.88%	44.38 %	0.85%	44.38%
Comp Mole Frac (Methanol)	0.05%	0.05%	0.00%	0.05%	0.05%	0.00%	0.05%	0.00%

APPENDIX B – LNG PRODUCTION DATA

Table B 1: Operating Conditions of LNG production process.

Name	Natural Gas	NG-1	Propane(C3)-3	Propane(C3)-4	NG-2	NG-3	C3-5	C3-6
Vapour Fraction	0.99	0.99	1.00	0.01	0.98	0.98	0.00	1.00
Temperature [C]	30.00	1.66	28.50	-0.02	-17.60	-35.80	-0.02	-0.02
Pressure [atm]	40.00	39.51	4.77	4.67	39.01	38.52	4.67	4.67
Molar Flow [kgmole/h]	59,078.60	59,078.60	597,100.00	597,100.00	59,078.60	59,078.60	589,637.88	7,462.12
Name	C3-7-NG	C3-8-NG	C3-9-NG	C3-10-NG	C3-11-NG	C3-12-NG	C3-13-NG	C3-13
Vapour Fraction	0.11	0.12	1.00	0.00	0.09	0.11	1.00	1.00
Temperature [C]	-18.59	-19.70	-19.70	-19.70	-37.03	-38.99	-38.99	-37.96
Pressure [atm]	2.53	2.44	2.44	2.44	1.25	1.15	1.15	1.15
Molar Flow [kgmole/h]	589,637.88	589,637.88	73,613.33	516,024.54	516,024.54	516,024.54	516,024.54	549,131.47
Name	C3-14	C3-15	C3-16	C3-17	C3-18	MR-14	MR-15	MR-16
Vapour Fraction	1.00	1.00	1.00	1.00	1.00	1.00	1.00	1.00
Temperature [C]	-5.83	-7.88	21.33	20.72	30.00	-45.00	73.20	30.00
Pressure [atm]	2.44	2.44	4.67	4.67	5.69	4.34	22.66	22.17
Molar Flow [kgmole/h]	549,131.47	646,087.96	646,087.96	665,653.42	665,653.42	117,116.13	117,116.13	117,116.13
Name	MR-17	MR-18	MR-19	MR-1	C3-3-MR	MR-2	C3-4-MR	C3-5-MR
Vapour Fraction	1.00	1.00	1.00	1.00	1.00	1.00	0.18	1.00
Temperature [C]	62.90	30.00	59.62	30.00	28.50	1.69	-0.02	-0.02
Pressure [atm]	33.39	32.89	47.37	46.88	4.77	46.39	4.67	4.67
Molar Flow [kgmole/h]	117,116.13	117,116.13	117,116.13	117,116.13	68,553.42	117,116.13	68,553.42	12,103.33

Table B 2: Operating Conditions of LNG production process (cont.).

Name	C3-6-MR	MR-3	MR-4	C3-7-MR	C3-8-MR	C3-9-MR	C3-10-MR	C3-11-MR
Vapour Fraction	0.00	0.79	0.46	0.11	0.41	1.00	0.00	0.09
Temperature [C]	-0.02	-17.59	-35.68	-18.59	-19.70	-19.70	-19.70	-37.04
Pressure [atm]	4.67	45.89	45.40	2.53	2.44	2.44	2.44	1.25
Molar Flow [kgmole/h]	56,450.09	117,116.13	117,116.13	56,450.09	56,450.09	23,343.16	33,106.93	33,106.93
Name	C3-12-MR	C3.12-MR	1.00	2.00	C3-3	C3.3-MR	NG-4	NG-5
Vapour Fraction	0.69	1.00	1.00	1.00	0.00	0.00	0.00	0.00
Temperature [C]	-38.99	-22.20	30.00	30.00	0.66	0.66	-135.28	-154.64
Pressure [atm]	1.15	1.15	5.69	5.69	4.77	4.77	33.06	28.13
Molar Flow [kgmole/h]	33,106.93	33,106.93	68,553.42	597,100.00	597,100.00	68,553.42	59,078.60	59,078.60
Name	MR-4-V	MR-4-L	MR-5-L	MR-5-V	MR-6-V	MR-7-V	MR-9-V	MR-10-V
Vapour Fraction	1.00	0.00	0.00	0.00	0.00	0.03	0.03	0.32
Temperature [C]	-35.68	-35.68	-134.30	-130.00	-157.10	-158.31	-158.31	-139.60
Pressure [atm]	45.40	45.40	40.86	40.86	35.92	5.33	5.33	4.84
Molar Flow [kgmole/h]	53,484.00	63,632.13	63,632.13	53,484.00	53,484.00	53,484.00	53,484.00	53,484.00
Name	MR-7-L	MR-11	MR-12	MR-13	LNG	BOG	LNG 2	LNG -2
Vapour Fraction	0.02	0.15	0.15	1.00	0.05	1.00	0.00	0.10
Temperature [C]	-133.88	-135.33	-135.33	-45.00	-160.54	-167.84	-167.84	-167.84
Pressure [atm]	4.84	4.84	4.84	4.34	1.05	0.56	0.56	0.56
Molar Flow [kgmole/h]	63,632.13	117,116.13	117,116.13	117,116.13	59,078.60	5,621.49	53,457.11	59,078.60
Vapour Fraction	1.00	0.05						
Temperature [C]	-168.53	-175.36						
Pressure [atm]	0.26	0.26						
Molar Flow [kgmole/h]	5,621.49	53,457.11						

Table B 3: Compositions of main streams in LNG production.

Name	LNG	BOG	LNG 2	LNG -2	BOG 2	LNG (2)
Comp Mole Frac (Methane)	96.17%	100.00%	95.76%	96.17%	100.00%	95.76%
Comp Mole Frac (Ethane)	1.73%	0.00%	1.91%	1.73%	0.00%	1.91%
Comp Mole Frac (Propane)	0.59%	0.00%	0.66%	0.59%	0.00%	0.66%
Comp Mole Frac (i-Butane)	0.20%	0.00%	0.23%	0.20%	0.00%	0.23%
Comp Mole Frac (n-Butane)	0.18%	0.00%	0.20%	0.18%	0.00%	0.20%
Comp Mole Frac (i-Pentane)	0.10%	0.00%	0.11%	0.10%	0.00%	0.11%
Comp Mole Frac (n-Pentane)	0.07%	0.00%	0.08%	0.07%	0.00%	0.08%
Comp Mole Frac (n-Hexane)	0.10%	0.00%	0.11%	0.10%	0.00%	0.11%
Comp Mole Frac (n-Heptane)	0.61%	0.00%	0.68%	0.61%	0.00%	0.68%
Comp Mole Frac (n-Octane)	0.20%	0.00%	0.23%	0.20%	0.00%	0.23%
Comp Mole Frac (n-Nonane)	0.03%	0.00%	0.03%	0.03%	0.00%	0.03%
Comp Mole Frac (n-Decane)	0.00%	0.00%	0.00%	0.00%	0.00%	0.00%
Comp Mole Frac (H2O)	0.00%	0.00%	0.00%	0.00%	0.00%	0.00%
Comp Mole Frac (Nitrogen)	0.00%	0.00%	0.00%	0.00%	0.00%	0.00%